INITIAL RESULTS FROM THE HOUGHTON COLLEGE CYCLOTRON

By

Andrew J. Loucks

A thesis submitted in partial fulfillment of the
requirements for the degree of

Bachelor of Science

Houghton College

June 2007

Signature of Author.....
Department of Physics
June 22, 2007

.....
Dr. Mark Yuly
Professor of Physics
Research Supervisor

.....
Dr. Brandon Hoffman
Professor of Physics

INITIAL RESULTS FROM THE HOUGHTON COLLEGE CYCLOTRON

By

Andrew J. Loucks

Submitted to the Department of Physics
on 22 June 2007 in partial fulfillment of the
requirement for the degree of
Bachelor of Science

Abstract

Initial performance characteristics for the Houghton College cyclotron have been measured. The cyclotron consists of a cylindrical vacuum chamber with diameter 15.3 cm and height 2.5 cm containing a hollow "dee" electrode and a ground electrode. At resonance, an RF source that can be tuned to frequencies between 2 MHz and 15 MHz creates an oscillating electric potential of several thousand volts between the electrodes. The chamber is placed between the 15.3 cm diameter poles of a 1.1 T electromagnet and is evacuated to a pressure of about 10^{-6} torr. Hydrogen, helium, and deuterium gas may be introduced and ions created by electron bombardment from a hot cathode. The magnetic and oscillating electric fields cause the ions to spiral outwards, gaining energy as their orbit radius increases. We anticipate maximum kinetic energies for protons, deuterons and helium nuclei to be about 280 keV, 140 keV, and 70 keV respectively.

Thesis Supervisor: Dr. Mark Yuly
Title: Professor of Physics

TABLE OF CONTENTS

TABLE OF FIGURES

Chapter 1

INTRODUCTION TO THE CYCLOTRON

1.1 Introduction

In 1919 Ernest Rutherford performed an experiment [1] that led physicists in a new direction. By using alpha particles emitted from a naturally occurring radioactive isotope (radium C, now known as ^{214}Bi), Rutherford transmuted nitrogen into oxygen, becoming the first true alchemist. This experiment sparked a competition among physicists to create high energy particles because, according to Rutherford, "if α particles-or similar projectiles-of still greater energy were available for experiment, we might expect to break down the nucleus structure of many of the lighter atoms."[2] By doing this, physicists would gain a better understanding of the nature of matter on the atomic and nuclear scales. At first, it was expected that these particles would require energies of at least megaelectronvolts (MeV) in order to overcome the large potential barrier due to the positive charges in the nucleus. In order to penetrate the nucleus, a positively charged particle would need to have enough energy to overcome this barrier.

In 1928, a new theory [3] was proposed by George Gamow; it predicted from quantum mechanics that through potential barrier penetration, disintegration of some light elements might be achieved with charged particles having energies of 500 keV or less. Quantum mechanically, there is a very small probability that the particle could tunnel through the potential barrier presented by the electrical charge of the nucleus. In quantum mechanics, a particle can be described with a wave function which, when it encounters a potential barrier, decreases exponentially. Thus, if there are a large number of particles, a fraction of them may tunnel through the barrier and penetrate the nucleus, precipitating a nuclear reaction.

Over the next few decades, various attempts were made to accelerate subatomic particles artificially by using a large electric potential difference across an accelerating gap. In 1929 a professor at the University of California, Ernest Lawrence, devised a particle accelerator, the cyclotron, which could accelerate particles to high energies without the use of high voltages. A cyclotron accelerates positive ions by manipulating them in an electromagnetic field. Figure 1 illustrates this technique.

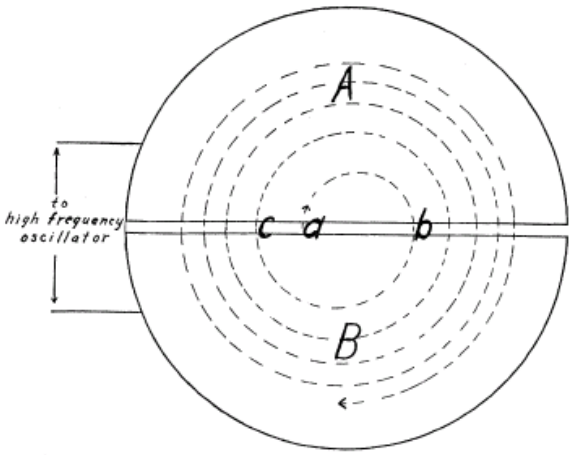

Figure 1. Concept of the cyclotron. As a positively charged particle starting at point a is accelerated between the dees A and B, its path is bent by a magnetic field pointing out of the page (not shown), resulting in the spiral trajectory shown by the dashed line. Figure taken from Ref. [4].

The cyclotron operates by applying a large radiofrequency voltage across two hollow electrodes (called "dees" for their shape) that are semi-cylinders, with their diameter much larger than their height. The dees are placed in an evacuated chamber and a low-pressure gas is introduced and ionized. The now positively charged ions are accelerated (in the gap between the dees) alternately toward one of the dees, and then the other, by the oscillating voltage on the dees. The polarity of the dees must switch while the particle is inside the dee, because inside of a conductor there is no electric field. If the chamber is now placed into a magnetic field that is orthogonal to the plane of motion, the particles' trajectories will be bent into a circle. The end result is the particles spiral outwards, gaining energy as their orbit radius increases. The radius of the particle's trajectory, and hence the circumference of the orbit, increases along with the particle's velocity in such a way so as to keep the time required for an orbit

constant. Thus the frequency of the oscillating potential on the dees is, fortunately, a constant frequency, called the "resonant frequency." When a particle is being accelerated in this way, it is said to be in "resonance." In this way, high energy particles can be obtained with a relatively low voltage on the dees.

1.2 History

1.2.1 Particle Accelerators and Cyclotrons

All particle accelerators use electric fields to accelerate charged particles. The difficulty, according to Lawrence, the inventor of the cyclotron, seemed to be twofold: "(a) the production of high voltages, and (b) the development of accelerating tubes capable of withstanding such high voltages." [5] The cyclotron was one of the first attempts at a method of acceleration which avoided these problematic high voltages. At first, physicists attempted to use a large potential difference to accelerate charged particles.

The Tesla coil, which uses electromagnetic induction between two coaxial coils, was considered initially as a possible high voltage source. The primary circuit is an LC circuit, with a spark gap in series. A DC source charges the capacitor until the spark gap discharges, at which point, the LC circuit oscillates at the resonant frequency. When the primary coil oscillates, a high voltage signal is induced into the secondary coil. The use of this device in particle acceleration was investigated [6] at the Carnegie Institution of Washington, but the experimenters eventually decided to abandon the Tesla coil for high voltage production; however, their work on accelerating tubes was later used in many other particle accelerators [7].

Other early attempts to accelerate particles depended on creating large direct current (DC) voltages. The electrostatic generator, for example, generates large potentials by accumulating charge on a conductive sphere supported by an insulating column. At the base of the column, charge is sprayed onto a moving insulating belt, which then carries the charge into the field-free region inside the conducting sphere, where it is collected and travels to the surface of the sphere. The voltage on the sphere is limited only by corona discharge and insulation leakage. Robert Van de Graaff built an early

device [8] at Princeton University, capable of 1.5 MV between two spheres, one at negative potential, and one at positive potential. He later built larger generators at the Massachusetts Institute of Technology [9]. While more sophisticated accelerators can produce more energetic particles (the most advanced Van de Graaff generators can produce only about 10 MV), the Van de Graaff accelerator is still desirable in many applications because the beam energy is very constant, and the voltage can be easily controlled.

Other direct current accelerators depended on voltage-multiplier circuits to create high voltages. For example, the Cockcroft-Walton multiplier circuit is shown in Figure 2 along with an accelerating tube. In this circuit, an alternating current is rectified and multiplied by two parallel banks of capacitors connected by diodes. During one half cycle, the diodes force this AC voltage to charge the capacitors in parallel. On the other half cycle, the capacitors are discharged in series. In this way, the circuit can create voltages in the range of 1 MV, which is sufficient for nuclear disintegration experiments. However, development of direct current sources was limited by breakdown of insulation and discharging, so alternate methods were sought to create even higher energies.

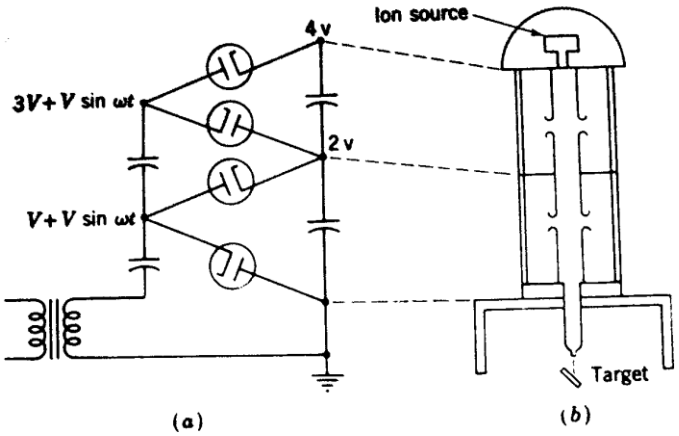

Figure 2. The Cockcroft- Walton multiplier used as a particle accelerator. It utilizes an AC input voltage, $V \sin(\omega t)$, which is multiplied and rectified by circuit (a). The ions are produced at the top of the accelerating column (b) and accelerated through the electrodes. The electrodes are powered from increasing voltage points from the Cockcroft-Walton multiplier. Figure taken from Ref. [10].

In 1924 Gustav Ising [11] published a paper describing an early linear accelerator which involved colinear cylindrical electrodes in a long evacuated tube through which the ions would pass (Figure 3a). A potential is applied as the ions pass through each electrode, causing them to accelerate as they pass out of each electrode. By having multiple electrodes, the ions can be accelerated multiple times by smaller voltage differences that "add" to obtain a higher energy. The voltage switching is timed by the lengths of wire connecting the power supply to the accelerating tubes (see the graph above the diagram in Figure 3a). The tubes further from the ion source (left of tube) need to be switched on later than the ones closer to the source, so the wires that connect to the later tubes are longer so that the ion reaches those tubes just as the signal does.

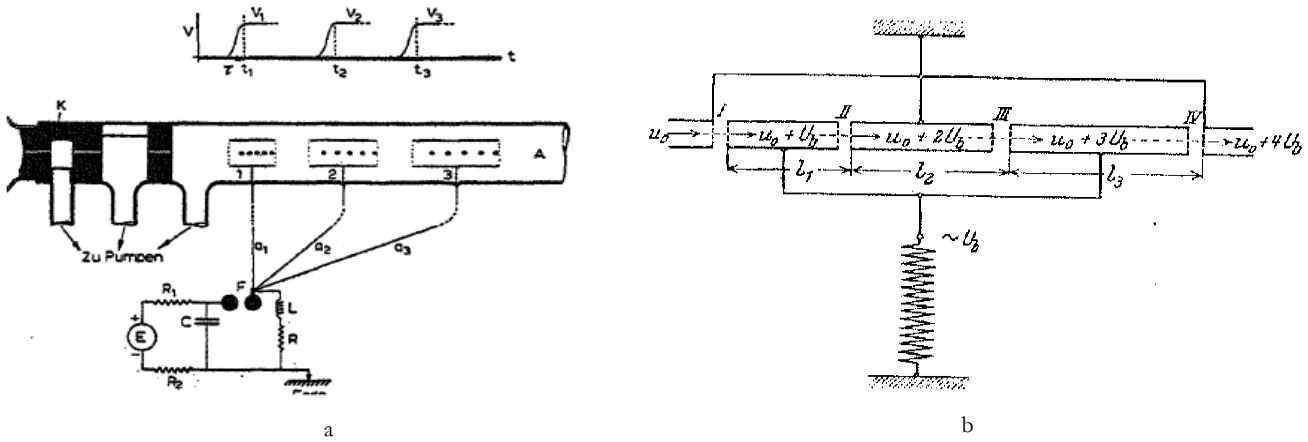

a b

Figure 3. Ising's (a) and Wideröe's (b) linear accelerators. Ions are accelerated in the gaps between electrodes. The mechanism that switches the voltages on the electrodes is different in each. In Ising's model, the lengths of wire time the voltage pulse, so that the voltage is applied just as the ions are leaving each particular electrode. In Wideröe's model, this is accomplished with an RF voltage applied to the electrodes, and the lengths of the electrodes increase to compensate for the increase in velocity. Figure (a) was taken from Ref. [12] and Figure (b) was taken from Ref. [13].

In 1928 Rolf Wideröe published a description of a working apparatus [14] using a radiofrequency voltage to prove the concept. In the working model, Wideröe used three cylindrical electrodes in a long vacuum tube. An RF voltage was applied to these electrodes such that, as the ions passed through

the electrodes, the voltage reversed polarity. Thus, the ions (in this case, potassium and sodium) accelerated between the first and central cylinder, and again between the central and final cylinder, giving a final energy twice that developed by one acceleration gap. In a linear accelerator that could produce ions with energies capable of nuclear disintegrations, many of these accelerating tubes must be used. In order to switch the polarity of the tubes at a fixed frequency as the particles accelerate, increasingly long accelerating tubes would be required, and thus very long vacuum chambers. Ernest Lawrence, the inventor of the cyclotron, worked with a student, D. H. Sloan, on an accelerator of this type using 30 electrodes, and achieved 1.26 MeV mercury ions[15].

In early 1929, Lawrence, a professor at the University of California, read Wideröe's paper [16]. He soon realized particle energies in the range desired (several MeV) could be achieved by modifying Wideröe's concept. Instead of using a long line of electrodes in succession, he explored the possibility of using the same electrodes multiple times with a magnetic field to send the ions back and forth between the electrodes. Lawrence and a graduate student, Nels Edlefsen built two small prototypes [17]; both were unsuccessful. Another graduate student, M. Stanley Livingston, undertook the project and it became the subject of his doctoral thesis [18]. The first working proof-of-concept model, only four and a half inches across, was completed in early 1931, and produced 80,000 eV protons with only a 1,000 volt RF signal on the dee [19]. It should be noted that, historically, cyclotrons were often named by the diameter of the electromagnet poles, which is the biggest limiting factor on their maximum energy. Work immediately began on a cyclotron capable of disintegrating nuclei, the 11-inch cyclotron [20], which was completed in 1932 and ultimately produced 1 MeV protons, the first machine capable of achieving this energy. In 1932, as this apparatus was being completed, Cockroft and Walton published their work [21] using a voltage multiplier as a particle accelerator. Using 400 keV protons, they were able to disintegrate lithium atoms, the first nuclear disintegration using a source of artificially generated high energy particles. Lawrence, Livingston and White quickly verified their results [22] with the 11 inch cyclotron.

Over the following decades, cyclotrons increased in size and particle energy, and were used to test models of the nucleus and explore interactions between particles. Soon followed the 27 inch [23], 37

inch [24], and 60 inch [25] cyclotrons at Berkeley, as well as many other installations at other universities and laboratories. These were the "first generation" cyclotrons that held the magnetic field and cyclotron frequency constant.

In 1938 H.A. Bethe [26] and M. E. Rose [27] published the results of a rigorous theoretical study to determine the maximum energy of the cyclotron, which is limited by relativistic effects on the mass of the particle. Because of relativistic mass effects, either the magnetic field or the frequency needs to change with orbit radius in order to maintain the cyclotron operation. J.R. Richardson, K.R. MacKenzie, E.J. Lofaren, and B.T. Wright demonstrated a frequency modulation technique [28] to correct for the relativistic effects on mass. Thus, the second generation of cyclotrons emerged, the synchrocyclotrons. The first of these synchrocyclotrons was the 184 inch cyclotron at Berkeley, on which completion was halted until after World War II. The third generation of cyclotrons came a decade later, in the 1950s. These Thomas cyclotrons (named for an early cyclotron engineer, L. H. Thomas), also called isochronous cyclotrons or azimuthally varying field cyclotrons, were able to achieve high energies with high intensity beams. In these cyclotrons, the relativistic increase was accounted for by varying the field of the magnet azimuthally, with alternating sectors of increasing and decreasing magnetic field. This allowed the particle beam to remain focused, while at the same time maintaining resonance for particles which increased in mass.

During this time period, two new types of accelerators were invented, the betatron and the synchrotron. The betatron was invented in 1946 by D. Kerst [29]. It accelerates electrons in a toroidal vacuum chamber using an electromagnet with a carefully shaped magnetic field. An AC voltage is applied to the electromagnet's coils and, during the quarter cycle when the magnetic field is increasing, it induces an electric field in the ring that accelerates electrons injected into the vacuum chamber. This same increasing magnetic field also holds the electrons in a circular orbit. The betatron is essentially a transformer, with the secondary coil being replaced by the electrons in the ring shaped chamber. In the 1960s, the synchrotrons became the accelerators of choice for high energy particle physics, and continue to accelerate to the highest energies. Synchrotrons are similar to cyclotrons; they accelerate particles by oscillating voltages along a path that is bent by a magnetic field. However, the frequency

and magnetic field are varied to keep the particles moving along a fixed path. Sometime in 2008, the Large Hadron Collider, a synchrotron, will be completed at the CERN in Europe, and will be the largest accelerator ever built, able to accelerate protons to 7 TeV.

1.2.2 Small Cyclotrons

Small cyclotrons have many design features and constraints in common. Many abandon the common two dee system described above in favor of using one dee. In fact, the first two cyclotrons built by Lawrence and Livingston used only one dee. In a one dee system, the high voltage radiofrequency signal is applied to a single dee, with the other being a grounded electrode, called a "dummy dee." In some cyclotrons, the dummy dee is neglected and the grounded chamber wall itself acts as a dummy dee. One dee is often preferred in small cyclotrons due to space constraints because, along with the electrodes, an ionizing source and a beam extraction system need to fit in the chamber. Small cyclotrons usually require some innovation, because there is little published on small cyclotrons, and because many small cyclotron builders are constrained by cost. In fact, these projects are often taken on by amateur science enthusiasts.

One of the earliest of these small machines was built in 1947 by four high school students at El Cerrito High School (in El Cerrito, CA), along with their teacher and some help from the nearby Radiation Laboratory at Berkeley. The El Cerrito cyclotron [30] [31] was completed in 3 months time (the project continued and was improved upon for years) for a cost of $600 (almost $6000 in 2006, adjusted for inflation). It was able to produce a 7 microampere beam of protons with energies of 1 MeV. It was built at a time when cyclotrons and accelerator physics were still new science. The El Cerrito cyclotron was the twenty-fifth completed cyclotron in the United States. For comparison with other small cyclotrons, this machine's magnet poles had a diameter of 6 inches. Initially, the students considered using the pole faces of the magnet as the top and bottom of the chamber, and then designed the chamber walls to be in two sections which clamped around the poles of the magnet. They also considered a glass chamber, but eventually settled on two circular steel plates that clamped on either side of a segment of brass tubing.

Another early small cyclotron [32] was built between 1954-7 at Iowa State University by undergraduate physics students. It utilized a magnet with 10 inch pole faces, and could accelerate hydrogen ions to 1.5 MeV with a maximum beam current of 2 microamperes. The cyclotron was intended to be the first cyclotron large enough to carry out nuclear research built and maintained by undergraduates. The ISU cyclotron made use of a current regulator, which stabilized the magnet current to within 4 gauss in a 17,000 gauss field. To measure the field strength, nuclear magnetic resonance was used. Powdered lithium, with a net magnetic moment, was placed in the field. In the presence of the magnetic field, the lithium atoms precessed at a frequency proportional to the magnetic field. A circuit was then devised which measured this frequency and adjusted the magnet current.

In 1981, researchers at Berkeley University built a small cyclotron called the "cyclotrino" [33], to be used in accelerator mass spectrometry (AMS). A sample was vaporized in the cyclotron, and the ions accelerated. From the cyclotron resonance condition, the charge to mass ratio of the ions can be found. This machine was specifically intended for carbon-14 dating [34]. Traditionally, this is done by counting the decay rate of the sample. However, for samples with a low count rate (very small or old samples), the sensitivity of the measurement is poor. AMS using a cyclotron was a solution that allowed for accurate measurements because, instead of counting decays, the amount of ^{14}C in a sample was measured directly. However, background ^{14}N interfered with measurements. The cyclotrino was an attempt to create an accelerator with excellent mass resolution that could accelerate negative ions because ^{14}N does not form a negative ion, but ^{14}C does, thus removing the background interference. The cyclotrino had a better mass resolution than conventional mass spectrometers because the radiofrequency signal was operated at odd high harmonics. As discussed previously, the cyclotron frequency is constant, and the polarity on the dees is switched while the particle is in the field-free region inside the dee. The frequency could also be such that, instead of switching once, it could switch any number of odd times, as long as it has the proper polarity when the particle approaches the gap between the dees. This greatly reduces the amount of time that the particle can be in the acceleration gap and still be accelerated correctly. Thus, if a desired particle is in resonance, and an undesired particle similar in charge-to-mass ratio is also being accelerated, the undesired particle will fall out of resonance more quickly if the frequency is operating at a higher harmonic. The cyclotrino operated

between the 11th and 15th harmonic and used a one dee system with a dummy dee. Electrostatic deflectors and mirrors were placed in the chamber to allow for the beam to enter and exit the chamber properly. This machine also utilized an external ion source with electrostatic lenses and filters. The beam path had a maximum radius of 10 cm, at which the energy of the particles was 40 keV.

One noteworthy small cyclotron was built by a high school senior, Fred Neill [35], in 1994. Every component was either surplus, salvage, or homemade; the vacuum system was built almost entirely from scratch. The magnet pole face diameter was 4.5 inches (the same as Lawrence and Livingston's first cyclotron), and the magnet could create a magnetic field of 0.67 T. Neill's first chamber design was unable to introduce low pressure gas, and so only accelerated air molecules. He later redesigned the chamber, using two dees, and accelerated hydrogen, helium, and magnesium ions. The resonant frequency of these ions agreed reasonably well with the expected values. He estimated the final energy for hydrogen ions was 70.5 keV (compare with 80 keV for the first cyclotron).

Rutger's University has completed two small cyclotrons [36] [37], a 9-inch, and a 12-inch cyclotron. Tim Koeth began the project in 1995, during his sophomore year of college. Koeth worked with Stuart Hanebuth on the nine inch cyclotron, achieving 600 keV protons in 1999. Eventually they acquired a larger magnet, and they constructed the 12 inch cyclotron (completed in 2001), capable of producing 1.2 MeV protons.

Finally, another small cyclotron [38] was built by Jeff Smith at Knox College as a physics honors project. The cyclotron was not completed because the wires that powered the ion source were bent by the magnetic field, which created a short circuit when they contacted the chamber wall. Since these wires carried a large current, they experienced a force when placed into the magnetic field. If the cyclotron was completed, the device could have accelerated protons to 1.5 MeV. It used a 2 Tesla magnet, with a pole face diameter of 8.9 inches, and featured a vacuum chamber containing two dees and provisions to allow for beam extraction.

1.2.3 The Houghton College Cyclotron

Work on the Houghton College Cyclotron began in the fall of 2001, with the goal of accelerating deuterons to be used to produce neutrons with the deuteron-deuteron fusion reaction. The neutrons, being highly penetrating would pass through the chamber wall and could be used for nuclear physics experiments. The original plan was to use a permanent magnet with a 6 inch diameter pole, which was capable of 0.5 T. Unfortunately, because it was a permanent magnet, it could not be turned off like an electromagnet, and so would attract tools and the iron end-plates of the chamber, which were difficult to get in and out of the magnet. In the spring of 2005, a commercial electromagnet with a 6 inch pole face, capable of up to 1.1 T, was acquired. The chamber design used a strip of brass rolled and soldered into a thin ring with two thick brass rings of larger diameter soldered to the top and bottom of the thin ring to create flanges. Plates would then be screwed to the top and bottom of the chamber, and o-rings would be used to create a vacuum seal. Soft iron and glass were considered for the plates, but aluminum was chosen. Soft iron is ferromagnetic, so if it were used for the plates, it would act as an extension of the magnet pole, and effectively shorten the pole gap, increasing the magnetic field. This would, however, shape the field, possibly in an undesired way.

Most of the earliest work on the cyclotron centered on the vacuum system, which was finally completed and tested in the fall of 2004. During this time, a water chiller (used to cool the magnet and the diffusion pump) was installed, and electrical controls for the vacuum system were also devised. The vacuum system consists of a rotary forepump, a diffusion pump, and a liquid nitrogen cold trap, as well as gauges to measure the pressure and vacuum valves used to isolate elements of the system. With the vacuum system completed, the chamber and the dee and dummy dee electrodes were fabricated through 2005 and 2006. Finally, the RF system was completed, and in the spring of 2007 all the systems were tested simultaneously, producing a beam current of a few nanoamps.

Chapter 2

CYCLOTRON THEORY

The cyclotron operates by accelerating charged particles across the potential between two dee electrodes multiple times, by using a radiofrequency high voltage signal applied to the dees. In order to send the particles back and forth between the two dees, an external magnetic field perpendicular to the plane of motion of the particles is used to bend the particles' trajectory. As the particles pass through the gap, they are accelerated, and the radius of the orbit increases, so the particles' path becomes a spiral. In this chapter, this process will be given a quantitative treatment.

2.1 Cyclotron Frequency and Energy

To determine the frequency at which the polarity of the RF signal applied to the dees must switch, consider the motion of an ion of mass m and charge q in the cyclotron chamber, with the origin of a cylindrical coordinate system centered between the dees (Figure 4). The ion of charge q is moving tangentially with velocity $\vec{v}$ in an

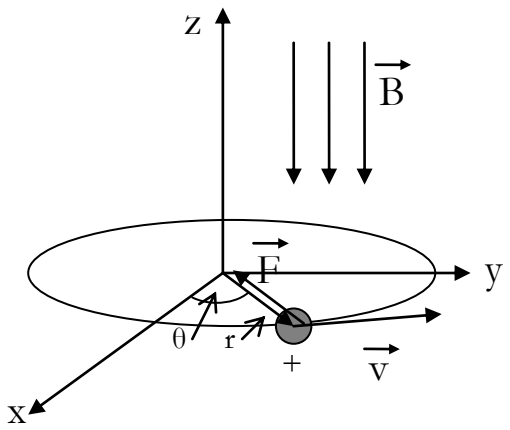

Figure 4. The motion of a positively charged particle, in the x-y plane, in a perpendicular magnetic field, $\vec{B}$, moving at a velocity $\vec{v}$ at a radius *r*, resulting in the centrally directed Lorentz force, $\vec{F}$.

orbit, where the central force responsible for the circular motion is the Lorentz force due to the uniform magnetic field $\vec{B}$, which is perpendicular to the plane of motion. According to Newton's second law,

$$\vec{F}_m = q\vec{v} \times \vec{B} = \frac{-mv^2}{r}\hat{r}\,. \tag{1}$$

Since $\vec{v}$, $\vec{B}$, and $\hat{r}$ are perpendicular, this reduces to

$$v = \frac{qBr}{m}\,. \tag{2}$$

The ion's velocity is equal to the distance traveled (the circumference) divided by the time required, or orbital period (T),

$$v = \frac{2\pi r}{T} = 2\pi r f\,, \tag{3}$$

where f is the orbit frequency, which using Equation (2) can be found to be

$$f = \frac{qB}{2\pi m}\,. \tag{4}$$

Thus, the frequency of revolution of the particle, and by extension the frequency that the voltage across the dees must switch polarity, is independent of the velocity or the radius of the orbit. This is because, as the velocity of the ion increases, the radius of the orbit increases in such a way as to keep the time required for an orbit constant. This is advantageous because it allows a cyclotron to operate at a constant frequency, given by Equation (4). A plot, showing this resonant frequency as a function of magnetic field for a few particles, is given in Figure 5.

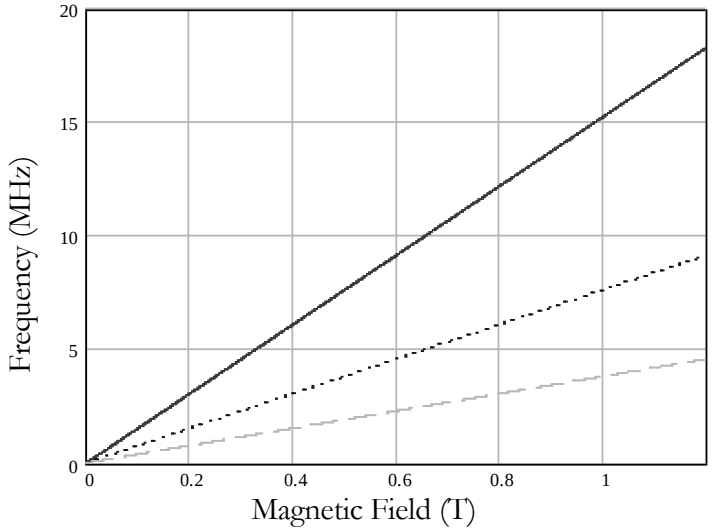

Figure 5. A plot of the cyclotron frequency as a function of magnetic field from Equation (4) for hydrogen (solid line), deuterium and doubly ionized helium (dotted line), and singly ionized helium (dashed line).

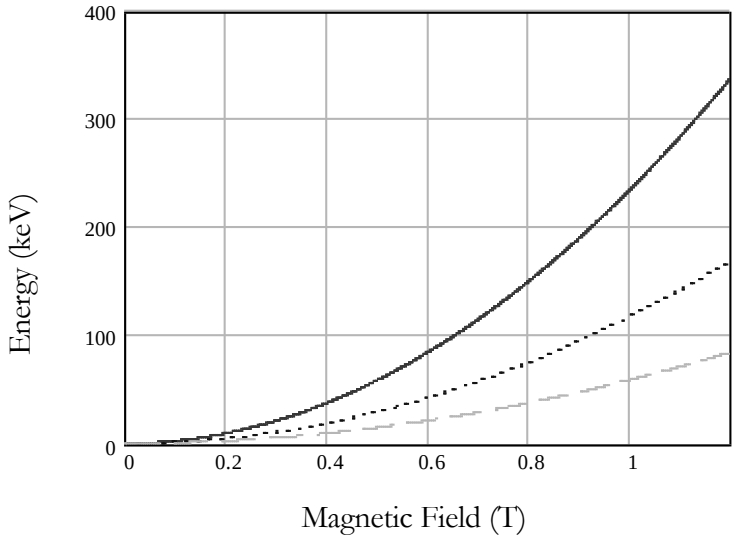

Figure 6. A plot of the maximum kinetic energy as a function of magnetic field from Equation (5) for hydrogen and doubly ionized helium (solid line), deuterium (dotted line), and singly ionized helium (dashed line), as a function of magnetic field strength. A value of 7 cm was chosen for the final radius, which is approximately the value in the Houghton College Cyclotron.

The final kinetic energy of the ion, as it reaches an orbit of radius R, can be determined from Equation (2) using the classical kinetic energy, $\frac{1}{2}mv^2$

$$T = \tfrac{1}{2}mv^2 = \frac{1}{2}\frac{q^2}{m}B^2R^2 . \qquad (5)$$

Note that because of the quadratic dependence on B and R, a small increase in the magnetic field or the final radius greatly increases the final energy of the ion (see Figure 6). This is why that the most significant constraint on the maximum energy obtainable is the magnet pole diameter, because once the iron magnet poles become saturated (at about 2 T [39]) the maximum energy is determined by R.

The kinetic energy given to a particle of charge q crossing an electric potential difference V is T = qV. Because this is done twice each orbit, the kinetic energy after N orbits is

$$T = 2NqV . \qquad (6)$$

From Equation (5), the orbit radius after N orbits is obtained.

$$r = \sqrt{\frac{4mNV}{q}}\frac{1}{B} . \qquad (7)$$

2.2 Electric and Magnetic Focusing

The previous treatment of the cyclotron assumes that the ion is traveling in a plane parallel to the dees and is perfectly synchronized so that it crosses the accelerating gap as the polarity switches. Furthermore, the effects of the fringes of the external magnetic and electric fields have not been considered. Consider the side view in Figure 7 of the ion traveling in a circle in a magnetic field. The force due to the magnetic field is perpendicular to both the magnetic field and the trajectory of the particle. The force due to the fringe magnetic field can be broken down into a radial component and a vertical component. The radial component is responsible for the particle continuing the circular trajectory; this is the component that was considered in the previous section.

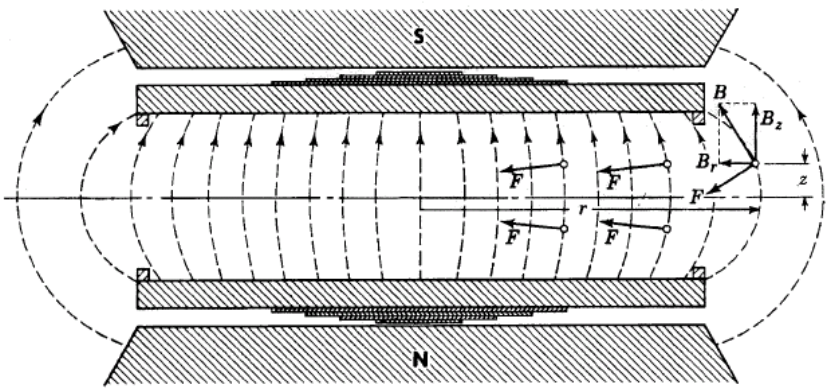

Figure 7. The effects of the fringe magnetic field on a positively charged particle traveling into the magnetic field (trajectory is into the page). Because the force exerted on the particle is normal to the magnetic field and the trajectory, the particle is forced to continue the circular path by the radial component of the magnetic field, and is forced back towards the central plane by the vertical component of the field. Figure taken from Ref. [40].

The vertical component of the force pushes the particle towards the central plane. Therefore, the fringe magnetic field focuses the ions that are not on the central plane by forcing them towards the central plane. This effect is stronger at greater radii because the fringe field is only significant at these greater orbit radii. This must be balanced with the consequences resulting from Equation (4). If the magnetic field decreases, then the resonant frequency of the particle changes, creating a phase difference between the dee frequency and the resonant frequency given in Equation (4). As long as this phase shift is small, then the particle will still be accelerated.

Now consider Figure 8, a side view of a positive ion traveling through the acceleration gap. The force due to the electric field is given by

$$\vec{F} = q\vec{E}\,, \tag{8}$$

thus the force points along the electric field lines. One can see from Figure 8 that as the particles enter the field they experience a force pointing them toward the central plane, resulting in a focusing effect.

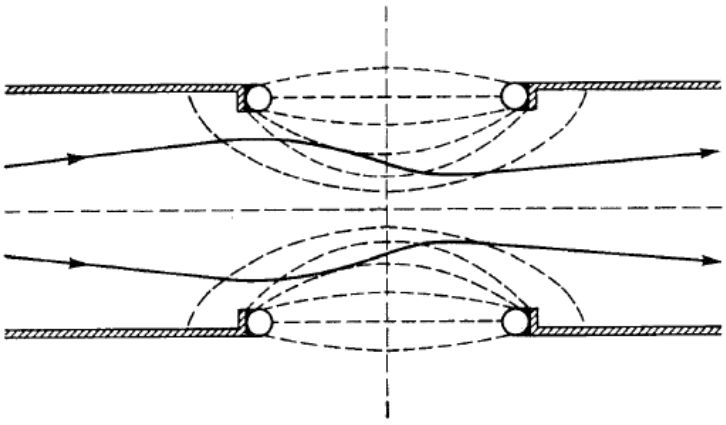

Figure 8. Cross sectional view of trajectory of positive ions across the acceleration gap between the dees. In this case, the dee on the right is at negative potential, and the dee on the left is at positive potential. The dotted lines represent the electric field lines. The accelerating gap creates an electric lens that focuses the charged particles in a manner analogous to an optical lens. Figure taken from Ref. [41].

As the particles exit the field, however, they experience a defocusing force. Because the particles are accelerated across this gap, they are moving slower in the focusing region, and thus are under the influence of the focusing force longer than in the defocusing region. The net effect is a more focused beam. The particles will be focused every time they pass through the accelerating gap. However, this effect will become negligible as the radius increases, because the particles are moving faster and spend less time between the electrodes. The net effect is the electric field focuses the beam at small radii, and the fringe magnetic field focuses at large radii.

In the original work done on the cyclotron by Livingston, these phenomena were stumbled upon by accident. In his recounting of the story [42], Livingston explained that in Lawrence's original concept, the electric field in the region inside the dees was zero, and the field was forced to be parallel to the central plane between the dees by a fine wire mesh over the open dee edge. While testing this, Livingston noticed very low beam currents, but on removing the wire mesh in pieces, the beam current improved. Upon Lawrence's return, he immediately realized this mechanism. Also, it was

discovered that making small adjustments to the shape of the magnetic field, or shimming, greatly improved the performance of the cyclotron.

2.2.1 Magnet Index

It is useful to consider the index of the magnet, n, when considering focusing and resonance. The vertical component of magnetic field can be parameterized by

$$\frac{B_Z}{B_0} = \left(\frac{r_0}{r}\right)^n, \tag{9}$$

where B_0 is the magnetic field at a radial distance r_0, and n is the magnetic field index. Solving for n yields

$$n = -\frac{r}{B_z}\frac{dB_z}{dr}. \tag{10}$$

This index determines how the ion will be deflected as the radius increases. As was discussed, in magnetic focusing the ion is forced toward the central plane and oscillates about it, at a frequency f_z. It was also shown in Equation (4) that the magnetic field affects the cyclotron frequency. In fact, an ion in this decreasing field undergoes radial oscillations about an equilibrium orbit, at a frequency f_r. Explicitly, these two frequencies are

$$f_z = \sqrt{n}\, f_0 \text{ and} \tag{11}$$

$$f_r = \sqrt{1-n}\, f_0, \tag{12}$$

where f_0 is the cyclotron frequency, given by Equation (4). A derivation of this result can be found in Ref. [43]. These results constrain the allowable values for n. If n is less than 0, then f_z is no longer real, so the particle no longer oscillates around the central plane, that is, it loses focusing, and likely collides with the top or bottom of the chamber or the dees. If n is greater than 1, then f_r is no longer real, and

the ion no longer oscillates radially, and falls out of resonance. Therefore, the value of n for the cyclotron must be between 0 and 1; it has been determined empirically the index should increase with r roughly linearly between 0 and 1 [44]. This can be accomplished by shaping the magnetic field by shimming the magnet; that is, by introducing ferromagnetic materials in a specific geometry between the pole face and the vacuum chamber. Finding the geometry can be accomplished experimentally, however, for a rigorous treatment of shimming, see Ref. [45].

2.3 Relativistic Effects and Maximum Energy

The fixed cyclotron frequency, Equation (4), assumes that the mass is constant. Once the particles achieve a high enough energy, this assumption becomes increasingly incorrect, because the mass increases. The relativistic resonant frequency can be found by considering the relativistic effects on mass. The relativistic mass, m, is related to the rest mass, m_0, according to

$$m = \gamma m_o , \tag{13}$$

where γ is the Lorentz factor,

$$\gamma = \frac{1}{\sqrt{1-\frac{v^2}{c^2}}} , \tag{14}$$

and where v is the velocity of the particle and c is the speed of light. The kinetic energy is the total energy less the rest energy,

$$T = mc^2 - m_0 c^2 . \tag{15}$$

Rearranging yields

$$m = m_o + \frac{T}{c^2}. \tag{16}$$

Using this and Equation (4), the cyclotron frequency becomes

$$f = \frac{qB}{2\pi m} = \frac{qB}{2\pi\left(m_o + \frac{T}{c^2}\right)}. \tag{17}$$

Therefore, the frequency is a function of T, which depends on R. Two solutions were presented [46] to account for this change in frequency, the Thomas cyclotron, and the frequency modulated cyclotron, or synchrocyclotron. The former, the Thomas cyclotron, uses a carefully shaped magnetic field. If the magnetic field increases with radius in order to balance the increase in mass, the particle will remain in resonance. However, it was shown in the previous section that beam focusing requires a magnetic field that decreases with radius. In order to account for these opposing constraints, the Thomas cyclotron uses a magnetic field that varies azimuthally, that is, evenly spaced radial sections decrease in magnetic field with radius, and in between, a magnetic field is increased with radius. This allows evenly spaced sections that focus but do not maintain resonance, and sections that maintain resonance but defocus the beam.

In the synchrocyclotron, the frequency is increased to match the increasing mass due to relativistic effects. In the synchrocyclotron, the frequency is ramped down according to Equation (17) so that one group of ions is accelerated to the exclusion of others. When the ions reach their maximum energy, the frequency begins the ramp again and accelerates another group of ions, so the resulting beam current is pulsed.

2.3.1 Maximum Energy of a Fixed Frequency Cyclotron

The fixed frequency cyclotron is limited by the relativistic increase in mass of the particle being accelerated. The low energy particles in the cyclotron are at the acceleration gap when the signal on the dees is at its peak. When the signal switches, the low energy particles are at the midpoint inside the

dees. The dees are being driven at a frequency given by Equation (4), which depends on mass. This frequency at relativistic energies becomes Equation (17). This leads to a phase shift between the dees' frequency and the orbit frequency of the relativistic particle. The relativistic particle will still be accelerated as long as the phase shift is less than $\pi/2$, because it will reach the acceleration gap between the signal switching and the peak. If the phase shift is greater than $\pi/2$, then it will reach the acceleration gap before the polarity switches, and be repelled, and fall out of resonance. Mathematically, this is written

$$\frac{\pi}{2} = \phi_0 - \phi = \omega_0 t - \omega t = 2\pi f_0 t - 2\pi f t \,, \tag{18}$$

where φ_0 is the phase, ω_0 the angular frequency, and f_0 the frequency that the dees are driven at. φ is the phase, ω the angular frequency, and f the frequency of revolution for the relativistic particle, and t is the total time the particle is being accelerated. Using the classical cyclotron frequency, Equation (4), and the relativistic cyclotron frequency, Equation (17), gives

$$\frac{\pi}{2} = qBt\left(\frac{1}{m_0} - \frac{1}{m_0 + \frac{T_m}{c^2}}\right), \tag{19}$$

where T_m is the maximum kinetic energy of the particle. Solving this for T_m,

$$T_m = m_0 c^2 - \frac{c^2}{\frac{\pi}{2qBt} + \frac{1}{m_0}}, \tag{20}$$

To find time t consider the particle as it drifts in the field free region inside the dee. The time it takes to traverse the path through one of the electrodes would be the distance (πr, because it is traversing a half circle) divided by its velocity,

$$t = \frac{\pi r}{v}. \tag{21}$$

Using Equation (2) gives

$$t = \frac{\pi m}{qB}. \tag{22}$$

Thus, the time it takes to drift through the dee is independent of the radius of the path or the velocity. To find the total time it takes it takes to travel through all the drift regions, this result is multiplied by the number of the total number of these drift regions, which is twice the number of orbits. The number of orbits decreases when the potential on the dees increase, so a larger potential on the dees results in a shorter total acceleration time. Taking Equation (20) into consideration, higher potential on the dees results in fewer orbits and a shorter time of acceleration, allowing for a higher maximum kinetic energy. Ref. [47] explores this topic more completely, and gives a maximum of 15 MeV for protons with 50 kV peak-to-peak across the dees.

2.4 Dee Voltage and RF System

The Houghton College cyclotron applies radiofrequency high voltage to the dee using the circuit in Figure 9. The dee and the walls of the vacuum chamber act like a capacitor. A resonant LC circuit is formed by adding an inductor. The inductor is energized by the driving circuit by a coil that is wrapped coaxially, and the two circuits are linked by mutual inductance. The LC circuit resonant frequency, if the mutual inductance is neglected, is given by

$$f_r = \frac{1}{2\pi\sqrt{L_2 C}}, \tag{23}$$

where L_2 is the inductance of the coil and C is the capacitance of the dee and chamber .

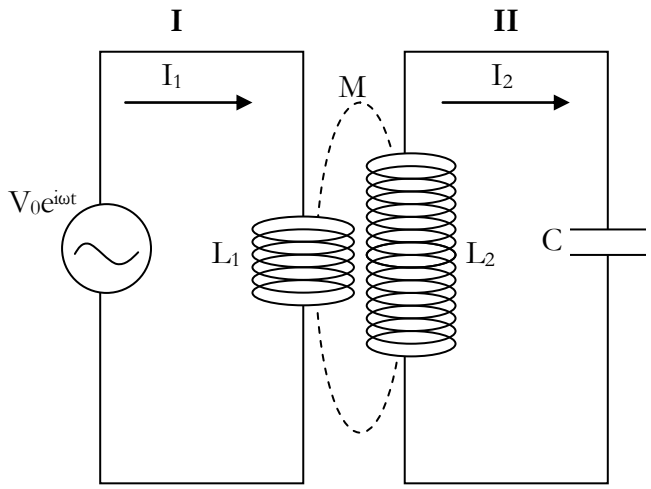

Figure 9. Simplified RF circuit. Circuit I drives the circuit II, the tank circuit connecting to the dee stem. L_1 is the primary coil, L_2 is the secondary coil, and M is the mutual inductance that links the two circuits. Assume some resistance in the wires, R_1 in the driving circuit, and R_2 in the LC circuit.

To calculate the voltage on the dees, consider this simplified circuit of the RF system. The calculations below follow closely those in Ref. [48]. Consider Kirchoff loops for the two circuits, and assume some resistance in the circuits,

$$R_1 I_1 + L_1 \frac{dI_1}{dt} - M \frac{dI_2}{dt} = V_0 e^{i\omega t}, \text{ and} \tag{24}$$

$$R_2 I_2 + L_2 \frac{dI_2}{dt} - M \frac{dI_1}{dt} + \frac{\int I_2 dt}{C} = 0, \tag{25}$$

where V_0 is the amplitude of and ω is the angular frequency of the RF voltage. I_1 and R_1 are the current and resistance in circuit I, and I_2 and R_2 are the current and resistance in circuit II, respectively. Solutions of theses differential equations for I_1 and I_2 are

$$I_1 = Ae^{i\omega t}, \text{ and} \tag{26}$$

$$I_2 = Be^{i\omega t}. \tag{27}$$

where A and B are the amplitudes of the currents. Substituting I_1 and I_2 into Equations (24) and (25) yields

$$A\left(R_1 + i\omega L_1\right) - iB\omega M = V_0, \text{ and} \tag{28}$$

$$B\left(R_2 + i\left(\omega L_2 - \frac{1}{\omega C}\right)\right) - iA\omega M = 0. \tag{29}$$

In general, impedance is defined to be

$$Z = R + i\left(X_L + X_C\right), \tag{30}$$

where the reactances are

$$X_L = \omega L \text{ and } X_C = \frac{1}{\omega C}. \tag{31}$$

Our expressions in Equations (28) and (29) can therefore be written in terms of the impedances,

$$AZ_1 - BZ_M = V_0, \text{ and} \tag{32}$$

$$BZ_2 - AZ_M = 0. \tag{33}$$

where Z_1 is the impedance in circuit I,

$$Z_1 = R_1 + i\omega L_1, \tag{34}$$

Z_2 is the impedance in circuit II,

$$Z_2 = R_2 + i\left(\omega L_2 + \frac{1}{\omega C}\right), \tag{35}$$

and Z_m is the impedance due to the mutual inductance,

$$Z_m = i\omega M\ , \tag{36}$$

Solving for A and B gives

$$A = \frac{V_0}{Z_1 - \frac{Z_M^2}{Z_2}}\text{, and} \tag{37}$$

$$B = \frac{V_0}{\frac{Z_1 Z_2}{Z_M} - Z_M}. \tag{38}$$

Using Equation (27) and this result, the current through the capacitor, I_2, can be found. The voltage across the capacitor, V_C, or the voltage on the dee, is the capacitive reactance times the current I_2. The denominator is complex, but can be made real by multiplying by the complex conjugate, so that V_C can be separated into real and imaginary parts. Explicitly, this is

$$V_C = Be^{i\omega t}X_c = \frac{V_o e^{i\omega t}}{\left(\frac{Z_1 Z_2}{Z_M} - Z_M\right)\omega C} = \frac{V_o e^{i\omega t}}{(\alpha + i\beta)\omega C} = \frac{V_o e^{i\omega t}}{(\alpha^2 + \beta^2)\omega C}(\alpha - i\beta), \tag{39}$$

where

$$\alpha = \frac{R_1}{M}\left(L_2 - \frac{1}{C}\right) + \frac{L_1}{M}\left(R_2 + \frac{1}{\omega C}\right)$$
$$\beta = \frac{\omega L_2 L_1}{M} - \frac{R_1 R_2}{\omega M} - \omega M \quad . \tag{40}$$

This can be written in the form

$$V_C = |V_C|\cos(\omega t + \varphi), \tag{41}$$

where

$$|V_C| = \frac{V_0}{(\alpha^2 + \beta^2)\omega C}\sqrt{\alpha^2 + \beta^2} \text{ and} \tag{42}$$

$$\varphi = -\tan^{-1}\left(\frac{\beta}{\alpha}\right). \tag{43}$$

2.5 Deuteron-Deuteron Interactions

The ultimate goal of the Houghton College cyclotron is to accelerate deuterons in order to produce neutrons using the $^2H + {}^2H \rightarrow {}^3He + n$ reaction. Deuterons from the cyclotron will become embedded in a target and react with later deuterons striking the target (Figure 10). The advantage to using the cyclotron to produce neutrons rather than charged particles is that a beam extraction system does not need to be devised because the neutrons will pass directly through the vacuum chamber wall. The calculations below follow closely those in Ref. [49].

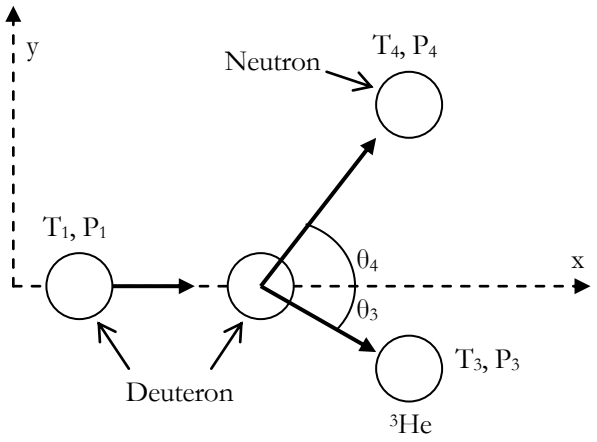

Figure 10. The D (d, n) ^{3}He reaction. A deuteron with kinetic energy T_1 and momentum P_1 strikes a deuteron at rest. Nuclear fusion takes place, resulting in ^{3}He with kinetic energy T_3 and momentum P_3 moving at an angle θ_3 with respect to the incident beam. A neutron is also given off at an angle θ_4 with energy T_4 and momentum P_4.

Energy is conserved, so

$$T_1 + Q = T_3 + T_4 \tag{44}$$

where Q is the energy released in the reaction, and T_1, T_3, and T_4 are the kinetic energies of the incident deuteron, the resulting neutron, and the resulting ^{3}He, respectively. Momentum conservation in the x direction and the y direction, respectively, are

$$P_1 = P_4 \cos\theta_4 + P_3 \cos\theta_3 \text{ and} \tag{45}$$

$$P_4 \sin\theta_4 = P_3 \sin\theta_3, \tag{46}$$

where P_1, P_3, and P_4 are the momentums of the incident deuteron, resulting neutron, and resulting ^{3}He, respectively. θ_3 and θ_4 are the angles at which the neutron and ^{3}He are moving, with respect to the central plane. For the D (d, n) ^{3}He reaction, Q = 3.268 MeV [50]. By squaring Equation (46), using the identity $\sin^2\theta_3 = 1 - \cos^2\theta_3$, solving Equation (45) for $\cos\theta_3$, and eliminating θ_3 gives

$$P_1^{\,2} = P_3^{\,2} + P_4^{\,2} - 2P_1P_4\cos\theta_4 . \tag{47}$$

Using the classical relationship between momentum and kinetic energy, $P^2 = 2mT$, Equation (41) becomes

$$m_1T_1 = m_3T_3 + m_4T_4 - 2\sqrt{m_1m_4T_1T_4}\cos\theta_4 \tag{48}$$

where m_1, m_3, and m_4 are the masses of the deuteron, neutron, and ^{3}He, respectively. Multiplying Equation (44) by m_3 and subtracting from Equation (48) yields

$$0 = T_1(m_3 - m_1) + T_4(m_4 - m_3) - 2\sqrt{m_1m_4T_1T_4}\cos\theta_4 + m_3Q , \tag{49}$$

which can be written as

$$T_4 - 2k_1\sqrt{T_4} - k_2 = 0 , \tag{50}$$

where

$$k_1 = \frac{\sqrt{m_1m_4T_1}}{(m_3 + m_4)}\cos\theta_4 \text{ and } k_2 = \frac{(m_3 - m_1)T_1 + m_3Q}{(m_3 + m_4)} . \tag{51}$$

The kinetic energy of the neutron can be found with the quadratic equation,

$$T_4 = 2k_1^{\,2} + k_2 \pm 2k_1\sqrt{k_1^{\,2} + k_2} . \tag{52}$$

If this equation is plotted as a function of angle θ_4, the result is Figure 11. The minus sign corresponds to a neutron with negative momentum scattered at an angle $\theta_4 + 180°$, and therefore is not a unique solution.

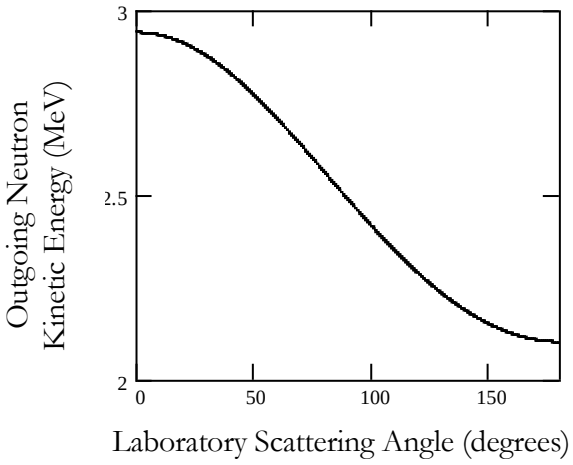

Figure 11. Kinetic energy of neutrons as a function of scattering angle for the D (d, n) ^{3}He reaction. The maximum neutron energy is 2.9 MeV and the minimum is 2.1 MeV, assuming 140 keV deuterons.

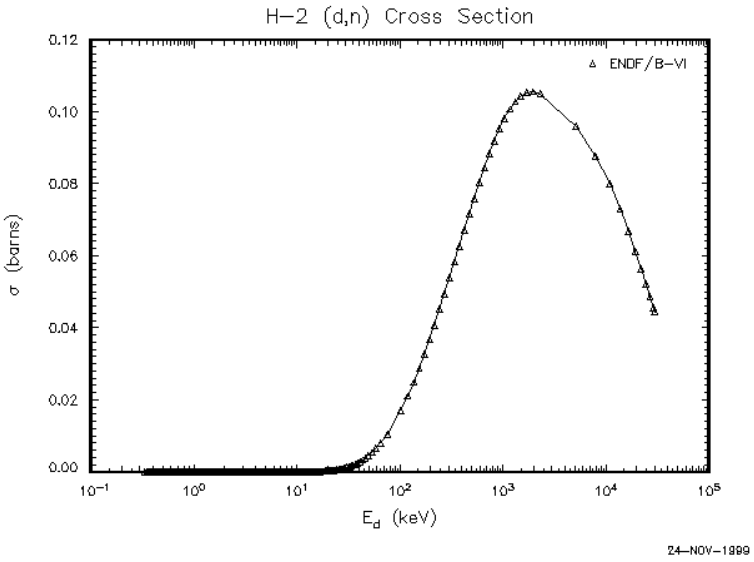

Figure 12. Cross sections for the D (d, n) ^{3}He reaction, as a function of incident deuteron energy. These data are from the B-VI library of the ENDF project [51].

Figure 12 shows a plot of the total cross section for this reaction as a function of incident deuteron energy. Cross-section (measured in barns) is proportional to the probability that a reaction will take place. For a deuteron with 40 keV incident energy, the cross-section is about 25 millibarns. For comparison, maximum cross section is about 105 millibarns at about 2 MeV.

The cross section can be used to find the reaction rate, or the neutrons produced per unit time, according to

$$R = \Phi \sigma N_A . \tag{53}$$

where R is the reaction rate, Φ is the incident deuteron beam intensity, σ is the total cross section, and N_A is the density of the target.

Chapter 3

DESCRIPTION OF THE CYCLOTRON

3.1 Overview

The Houghton College Cyclotron (Figure 13) is similar in scale to the original cyclotron built by Livingston [52], and consists of several systems which will be described below. The RF system supplies radiofrequency voltage to the dees which accelerate the particles, using the technique described earlier.

Figure 13. A photograph of the Houghton College Cyclotron. The electromagnet is prominent in the picture, with the chamber between the poles. The vacuum system is below the table on the right. Underneath the table on the left is the equipment for the RF system. The helium tank is also visible.

The Houghton College Cyclotron uses a system in which the radio frequency high voltage is applied to only one dee; the "dummy dee" electrode is grounded. These electrodes are in an evacuated chamber, which requires a system of pumps and valves. In order for the particles to orbit, the vacuum chamber is placed in an external magnetic field, provided by a commercial electromagnet. A gas handling system

and a hot cathode filament provide the ions. Once the ions are accelerated, they are collected on a target, and the beam current is measured.

3.2 Magnet

The magnet used for the Houghton College cyclotron is a GMW Associates 3473-70 Electromagnet, which has a pole diameter of 15 cm. Using a PowerTen R62B-4050 power supply at 50 A, the maximum magnetic field with a pole separation of 3.85 cm is 1.1 T. This magnet can produce higher fields (it can handle up to 70 A); however, the maximum field is limited by available water cooling and the power supply. A Haskris H-4057 water chiller, capable of 3.8 L/min (1.0 gpm) at 18°C, is used to cool the magnet and diffusion pump. Since the diffusion pump requires at least 0.8 L/min (0.2 gpm), the maximum that can be supplied to the magnet is 3.0 L/min (0.8 gpm). To achieve the maximum field, using 70 A, the magnet requires 6.1 L/min (1.6 gpm) of cooling water. Measurements of the magnetic field, made with an F.W. Bell 5070 Teslameter probe, at a pole separation of 3.85 cm, are shown in Figure 14 -16.

These data were collected using an aluminum disc (aluminum is non-magnetic), which rotated in a groove in a plastic disk that was centered on the magnet pole face. The height was such that the top of the disc was in the central plane between the poles. The aluminum disc had a groove milled in the top to accommodate the Hall Effect probe. An angular scale (marked on the aluminum disc) and a ruler were used to measure the field as a function of radial and angular position. Using the magnetic field measurements plotted in Figure 14 and Figure 15, the index of the magnet, Equation 12 was calculated (Figure 16). Because the radial measurements were recorded in increments of 1 cm, the dB_z/dr term was approximated by $\Delta B_z/\Delta r$, where Δr is the difference between two radii (1 cm), and ΔB_z is the difference between the axial magnetic field measurements at the two radii. The data points should be between 0 and 1 inside the chamber to maintain resonance and focusing, and should rise roughly linearly. The shape of this plot can be altered to give a linear dependence of n on radius by shimming the magnet, which should increase the beam current measured because fewer particles will fall out of resonance or focus.

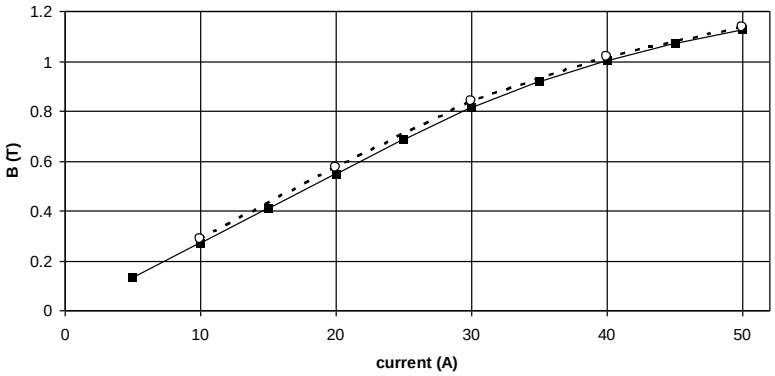

Figure 14. Plot of the measured (solid) and nominal (dashed) magnetic field as a function of current. The probe was placed in the center of the poles in the central plane at the center, with a pole separation of 3.85 cm.

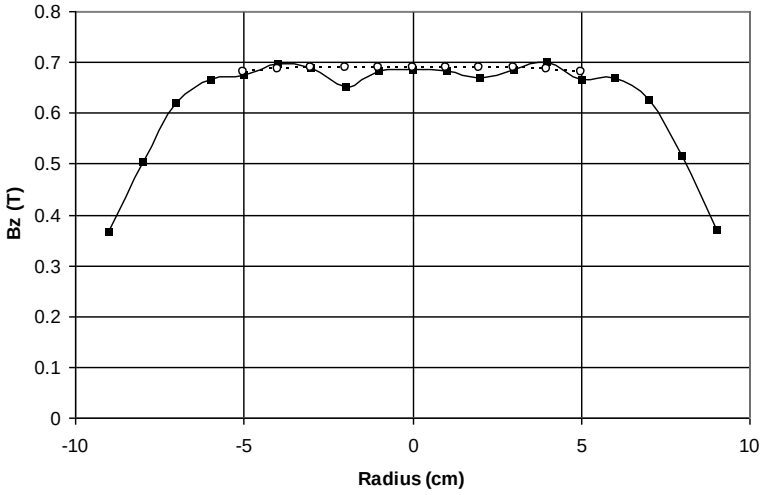

Figure 15. Measured (solid) and nominal (dashed) vertical component of magnetic field as a function of radius in the central plane of the magnet at 25 amps. The fluctuations in the measured field are most likely due to the method by which it was measured.

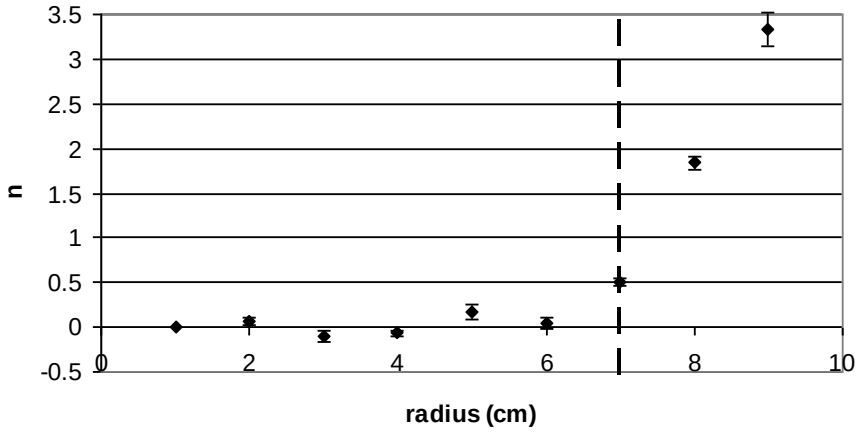

Figure 16. A plot of the approximate magnetic field index, n, versus the radius. The dashed line represents the edge of the dee electrode, approximately 7 cm. Ideally, this plot should increase between 0 and 1 linearly from the center to the 7 cm radius.

3.3 Vacuum System and Chamber

3.3.1 Vacuum Chamber

The particles are accelerated in the vacuum chamber shown in Figure 18. It is constructed of a strip of brass that is rolled and soldered to make a ring that is 2.86 cm high and 0.11 cm thick, with an inside diameter of 14.92 cm. Two brass rings (each has a height of 0.86 cm and thickness of 0.77 cm, with an inside diameter of 15.03 cm) are soldered to the top and bottom of this ring to form flanges. This arrangement makes up the chamber wall. To make the top and bottom lids for the chamber, 8 holes were drilled around the edge of two aluminum plates 18.0 cm in diameter and 0.72 cm thick. The holes in the bottom plate are tapped so that 8 brass screws can be used to sandwich the two plates with the chamber wall in between. The plates and the wall are sealed using two Viton O-rings, which fit into grooves milled into the plates. The top plate is milled to be only an eighth inch thick at the center on the inside to allow for more room for the filament. In the chamber wall, eight holes for ports are drilled, and brass QF-16 flanges are soldered in place. These allow for the following attachments: two glass viewports, the dee feed-through/stem, the vacuum system, the gas inlet, the beam collector, and the filament feed-through.

Inside the chamber, the dee and dummy dee must be isolated from the chamber wall and each other. The dee is suspended by the dee feed-through and attached to the dee stem with a small screw. In addition, glass slides are inserted between the bottom plate and the dee to provide extra support. The dummy dee is attached to the dee by glass slides attached to the dee and dummy dee with Loctite 1C high-vacuum epoxy. The dee is made from two semi circular pieces of copper soldered to a flat strip of copper. It has a diameter of 14.24 cm, a height of 1.57 cm, a length of 6.8 cm, and a thickness of approximately 0.09 cm. The dummy dee is a strip of copper bent into a rectangle, and soldered together; it is 14.45 cm long, 0.83 cm wide, and 1.6 cm high. It is separated form the dee by about 0.77 cm. The dee is separated from the chamber wall by about 0.34 cm.

Another glass slide (2.20 cm by 4.46 cm) is attached to the top of the dee, and two barrel connectors are attached to the top of the glass with epoxy. The filament is connected to these barrels. Two wires are soldered to an 8 pin feed-through, and connect to the filament via the barrels. A third wire connects from the feed-through to the dummy dee via a barrel. These connections allow for the filament to be powered, and for the dummy dee to be grounded.

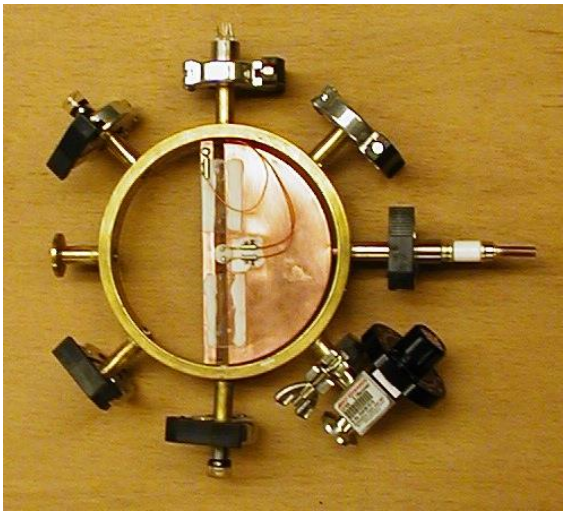

Figure 17. Photograph of the chamber with the lids removed, and with the filament feed-through, dee stem, needle valve, and glass viewports attached.

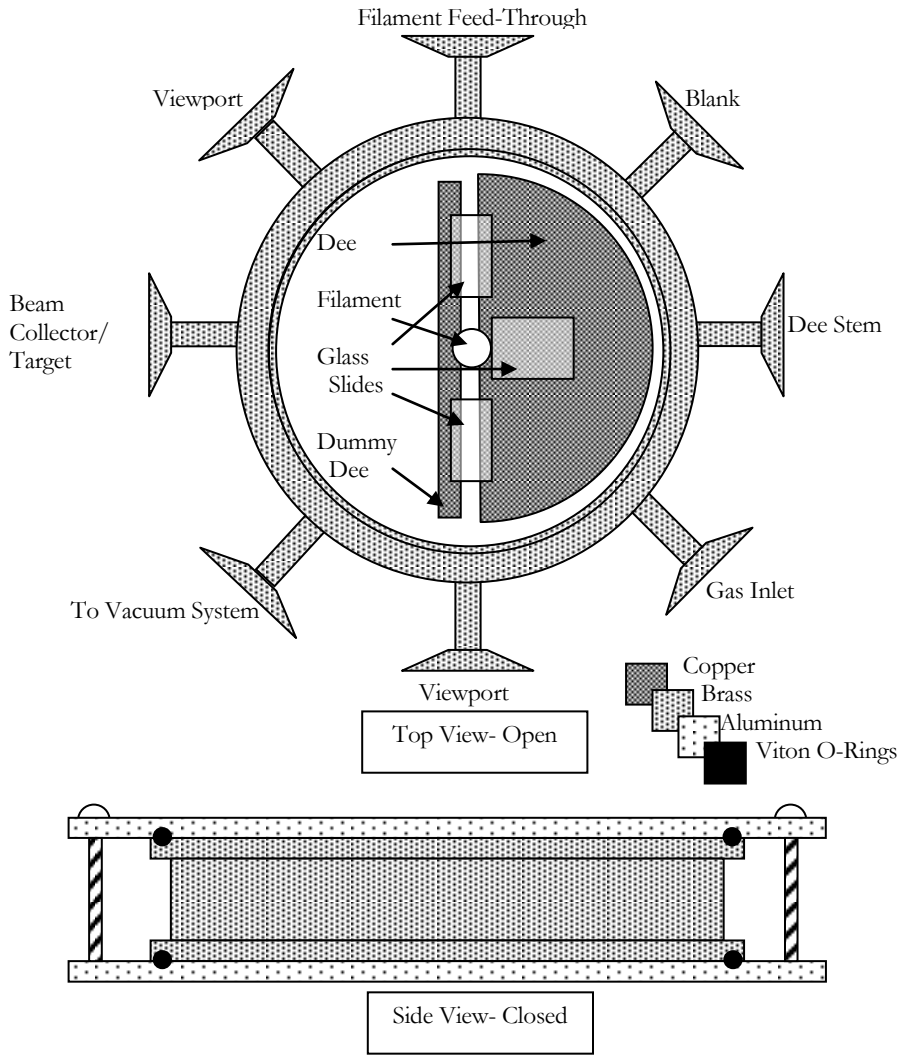

Figure 18. The Vacuum Chamber. Above is a top view with the lids removed; below is a side view with the plates attached by screws, without the side ports. The O-rings can not be seen, but are shown in their approximate position in a cut away.

3.3.2 Vacuum Pumps

The vacuum system maintains a low pressure inside the chamber. A CIT- Alcatel 2012A fore pump removes air from the chamber and vacuum system by compressing it into a reservoir, where it is allowed to escape through a one way valve. In this way, the pressure in the chamber can be reduced to

about 10^{-1} Pa (10^{-3} torr). To further reduce the pressure, an Innovac R220 diffusion pump and Kurt J Lesker TNR6XA150QF cold trap are used, which can lower the pressure to about 10^{-4} Pa (10^{-6} torr).

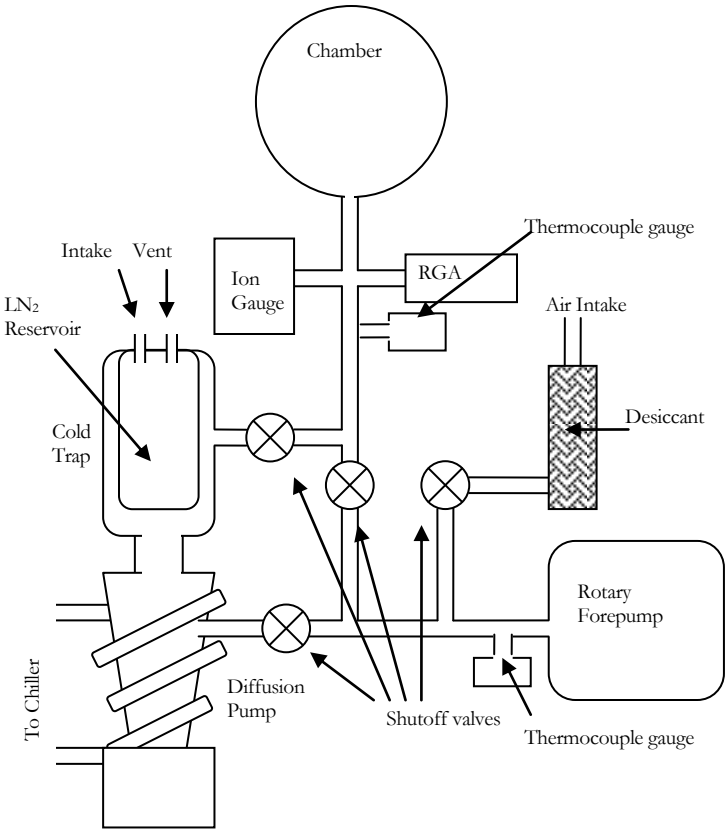

Figure 19- Schematic of the vacuum system. The shutoff valves allow elements of the system to be isolated while the rest of the system is evacuated. The foreline was constructed out of soldered copper pipe that was soldered together. The pressure can be measured with thermocouple gauges at higher pressures, and the ion gauge at lower pressures. The residual gas analyzer (RGA) can be used to determine the partial pressures of the residual gasses.

The diffusion pump operates by heating Dow Corning 704 Diffusion Pump oil in the base of the pump. The oil vaporizes, and rises up a central column in the pump. The vaporized oil is then forced downward through jets, which transfers momentum to air molecules. The walls of the pump are cooled by water, condensing the oil and returning it to the reservoir. The cold trap is filled with liquid nitrogen, which removes kinetic energy from particles, making it difficult for them to escape back into

the chamber. It also prevents the vaporized oil from streaming back into the chamber. The pressure is measured using two Granville Phillips CVG101GA thermocouple gauges, which read pressures as low as 10^{-3} torr in the chamber and fore line. They are ineffective at lower pressures, so a Granville Phillips 1-100-K Ion Gauge measures pressures down to 10^{-8} torr. The thermocouple gauge that reads chamber pressure and the Ion Gauge are both controlled by a SRS IGC100 Ion Gauge Controller. Also, a SRS RGA 100 Residual Gas Analyzer is used to determine the partial pressures of the gasses in the chamber.

3.4 Radiofrequency High Voltage Supply

The cyclotron requires the voltage on the dees to oscillate at frequencies in the megahertz range. The voltage must at least several thousand volts, otherwise, the ions must go through too many revolutions to reach the outer edge of the dee, which would increase the phase shift due to the fringe magnetic field and increase the probability that they would collide with residual gas molecules. The RF signal is produced by a HP 33120A function generator, a Kalmus 155LCRH RF power amplifier, and an LDG AT200PC antenna tuner, which is coupled to the cyclotron dee stem by two coils linked by mutual inductance (Figure 20). The function generator, amplifier, and tuner are connected to the driving coil, made of 6 turns of 12 gauge copper wire. The secondary coil is a General Electric 1 – 25 μH roller coil variometer, or variable inductor, which is connected directly to the dee, creating a resonant LC circuit, as described in Section 2.4. The variable inductor can be set at a value to match the capacitance of the dee in order to drive the circuit at a desired frequency, according to Equation (25).

The tuner cannot be connected directly to the dee stem because of the large capacitive load of the dee. Two mutually inducting coils are used to roughly balance the capacitive load, creating a resonance curve with a high quality factor (the quality factor is a term to describe how the sharp the resonance peak is). The coils are mounted in a metal box (to avoid accidental radio transmission), and the tuner is able to match the output impedance of the RF amplifier to the input impedance of the driving coil, thereby reducing the reflected power.

The connection to the dee stem from the coil box is crucial; it must have as little resistance as possible for a sharp resonance. The dee stem enters a large diameter coaxial transmission line. A cylindrical piece of brass stock 12.8 cm long and 5.1 cm in diameter was drilled to accommodate the dee stem. This hole was drilled so that it goes almost all the way through, and a very small hole in the other end accepts the pin on a UHF panel connector, to which it is soldered. UHF connectors are used because the output from the tuner is UHF, and the high voltage transmission (RG8X) cables have UHF connectors. The UHF panel connectors used had a ridge that roughly fits a 3/8" copper pipe. A piece of flat copper stock was cut to the size of the panel connector, and holes drilled and tapped so that the piece can be screwed to the panel connector. The center of this piece was drilled to accommodate the 3/8" side of a 3/8" to 1/2" copper pipe converter and is soldered in place. A 3/8" copper pipe fits snugly over the grounded connection on the dee stem and forms the outer, grounded shield for the coaxial transmission line. To allow for enough room for the central conductor, a 3/8" to 1/2" copper pipe adapter is slid over this connection, and connected to the other converter with a 5.97 cm long piece of 1/2" copper pipe.

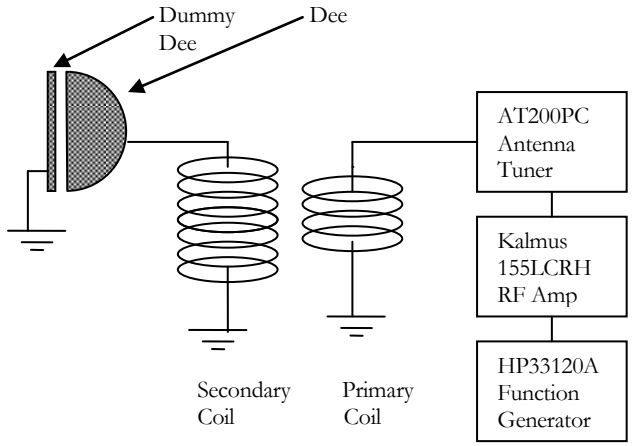

Figure 20. RF System. The function generator and RF amplifier are connected with RG58 coaxial cable. The RF amplifier, the antenna tuner are connected with RG8X coaxial cable.

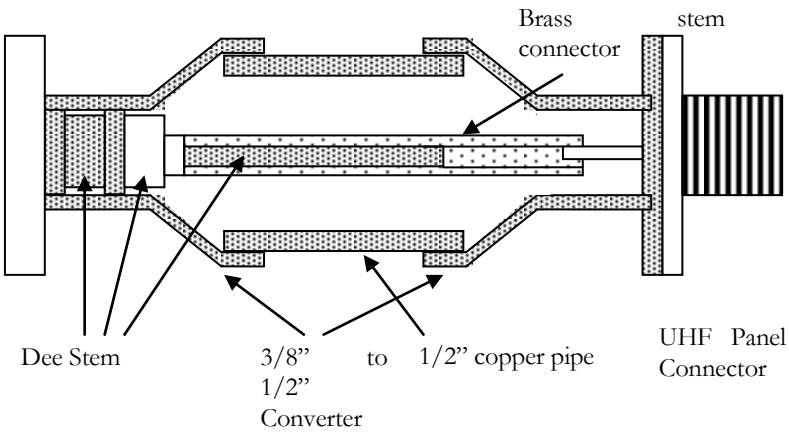

Figure 21. Cutaway of the dee stem connection. The central dee stem slides into the brass connector, which is soldered to the pin on the UHF panel connector. The copper converters and pipe make a grounded shield for this transmission line. By constructing the dee stem in this way, it is easily disassembled. All the pieces slide off except the UHF connector.

It is necessary to select an appropriate inductance for the variable inductor, which depends on the desired resonance frequency. For testing, it was decided to use helium, with two ionization states. When beam current is plotted as a function of magnetic field there should be two peaks, which would allow the cyclotron to be calibrated. For the radius of our cyclotron, it was found that both He^{++} with a magnetic field of 0.5 T and He^{+} with a magnetic field of 1.0 T have resonant frequency of 3.81 MHz. Note that the dee and vacuum chamber form a capacitor, with a measured capacitance of about 88.5 pF (the dee stem and assembly contribute to this capacitance). For an LC circuit, the resonant frequency is approximately given by Equation (23), requiring an inductance of 22.2 μH to resonate at 3.81 MHz.

3.5 Other Systems and Considerations

In addition to the primary components described above, several other systems are required for a working cyclotron. These are the water chiller, the gas handling system, the filament, the beam current collector, and the control system.

3.5.1 Water Chiller

The water chiller is a Haskris model H-4057. It can supply 1.0 gpm at 18°C. The water is pumped through polyethylene tubes, where it passes through a filter to remove particulates. The water also contains an algaecide. The chilled water is then diverted into two lines, one which flows into the magnet coils, and the other which flows to the diffusion pump. The quantity that flows in each line is controlled by two flow regulators, so that the magnet receives the required 0.8 gpm and the diffusion pump receives less than 0.2 gpm. Once the water passes through the magnet and pump, the lines join and return to the chiller.

3.5.2 The Gas Handling System and Ion Source

The gas handling system allows low pressure gas, currently helium, to be introduced into the system for ionization and acceleration. ¼" copper refrigerator tubing connects the helium cylinder to the valve system; a ball valve helium shutoff, a ball valve allowing for the line to be vented, and an Edwards LV10K fine control needle valve, which can admit helium at a rate that will maintain pressures as low as 8 x 10^{-6} torr. While this system allows helium to be admitted into the chamber, there is a significant amount of residual hydrogen remaining in the chamber most likely due to the stainless steel walls releasing hydrogen.

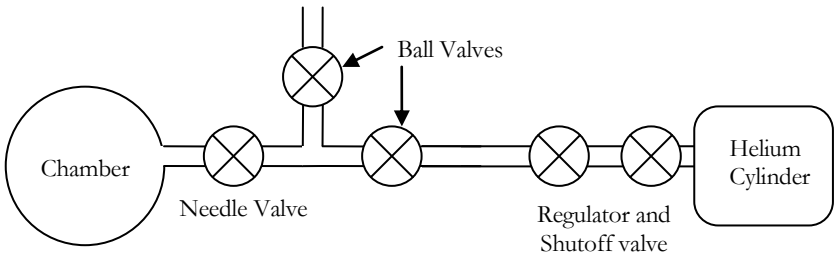

Figure 22. Gas Handling System. The regulator and the shutoff valve allow for the helium to be released from the tank. By opening both ball valves, the line is open to air, and the helium flushes air from the line. The top ball valve is then closed, and the helium is admitted into the chamber via the needle valve.

Once in the vacuum chamber, the gas is ionized by a hot filament cathode from an AEI type EM-6 electron microscope. The filament is mounted between the dee and the dummy dee, suspended from two barrel connectors mounted onto a glass slide on the dee. A current of about two amps causes the filament to glow, releasing electrons which strike the helium atoms, ionizing the gas. This filament is powered by a GW Instek GPS-3030DD DC power supply. This power supply floats at -100 volts (provided by a Keithley Instruments 240A high voltage supply) in order to repel the electrons (Figure 23a).

This ion source design presents a problem: the filament is in a magnetic field. As a current passes through the filament, a short section of the filament is perpendicular to the field (because of the shape, Figure 23b, it cannot be arranged so that it is entirely parallel to the field). Because of this, the magnetic field generates the Lorentz force on the moving charge of the current, which stresses the filament, and could break it. If, however, AC was used to heat the filament rather than DC, the force stressing the filament would not be applied long enough in one direction to break the filament. In order to generate a high frequency current of about two amps, a function generator, with a low current output, could be connected to a common-collector transistor power amplifier, which would amplify the current of the generator. If the gain of the amplifier is insufficient, a Darlington circuit could be used, which would essentially "piggyback" one transistor on another in a common-collector circuit, effectively doubling the gain of the amplifier.

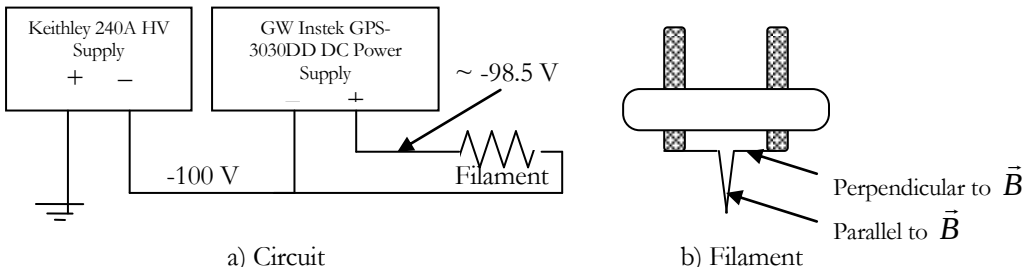

Figure 23. a) The filament power supply circuit. The high voltage supply floats the DC power supply at -100 V to repel electrons. The DC power supply gives about 2 amps at about 1.5 V. b) The filament is mounted on a ceramic disc with two pins passing through it. The filament itself is a fine wire mounted on the two pins, with a kink in it, which reduces the force due to the magnetic field and tends to emit electrons off the tip of the kink, acting as a point source.

3.5.3 Current Collector

The current collector is used to measure the beam current at various radii (Figure 24). The collector, a brass surface perpendicular to the particle beam, is suspended by an ceramic insulating column. The insulating column is attached to the bellows of a right angle Veeco valve, allowing the plate and column to be moved back and forth to intercept the beam at various radii. A shielded wire is soldered to the plate, and runs to a BNC Quick Flange feed-through, which connects to the Keithley 617 electrometer. Currently, of the beam collector is a brass plate that is perpendicular to the beam, attached to a screw with a hole drilled through its axis (in order to outgas the threads). This is screwed into a ceramic spacer, which connects to a grounded steel rod, which is screwed into the end plate of the bellows. The plate can intercept the beam between the radii of 4.66 cm and 6.00 cm. This collector will give poor accuracy because the beam impacting the collector can cause secondary electrons to be ejected from the metal surface, giving a false current measurement. A solution to this would be to have the current collector inside a conductive box with a narrow opening. The box would be kept at a negative potential, causing any secondary electrons to return back onto the collector.

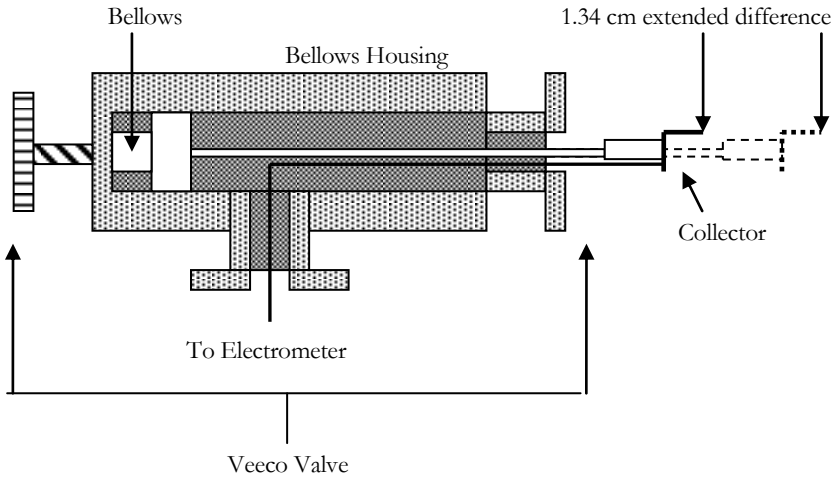

Figure 24. Existing construction of the current collector. The beam is intercepted by the collector, and the current is measured by a Keithley 617 electrometer. The radius that the collector intercepts the beam can be adjusted over a 1.34 cm range by turning the knob on the bellows.

3.5.4 GPIB Control System

It is desirable to control the cyclotron remotely, because the cyclotron will eventually be used to accelerate deuterons to produce neutrons, creating a radiation hazard. In addition to safety concerns, remote control will greatly improve the ease of operation. In order to control the various systems outlined, the General Purpose Interface Bus (GPIB or IEEE-488) communication interface will be used. This standard allows for up to 15 devices to share a single 8-bit bus with a maximum bit rate of 1 Mbps. The magnet power supply, ion gauge controller, RF function generator, and electrometer all can be controlled by GPIB. The filament also can be controlled over GPIB using a Unisource P6100 power supply instead of the GW Instek GPS-3030DD power supply to power the filament. The antenna tuner and RGA can be controlled by an RS-232 interface, which can be derived from GPIB using a National Instruments GPIB-232CV-A RS-232 to GPIB converter. All of these connections will be daisy-chained together and linked to a National Instruments GPIB-eNet GPIB/Ethernet converter, allowing the cyclotron to be controlled by a computer via the college's intranet, using a Labview program which has yet to be written.

Chapter 4

RESULTS

In this section, the results of testing the RF system, as well as the method of carrying out the measurements, will be given. In addition, preliminary results suggesting successful acceleration of protons will be shown.

4.1 RF Measurements

In the impedance matching circuit (Figure 20), the secondary coil's value was chosen by determining the desired resonant frequency and measuring the capacitance of the dee and chamber wall, according to Equation (23). For 3.65 MHz and a capacitance of 88.5 pF, ignoring the effect of mutual inductance in the LC circuit, an inductance of 21.4 μH was chosen for the secondary coil. The inductance of the primary coil which allows for the best power transfer was determined empirically.

This was done first by connecting the secondary coil to the dee, and placing a low amplitude oscillating signal directly on the primary coil using a HP 3310A function generator. A CalTest CT-2591 high-voltage oscilloscope probe was inserted through the gas inlet port when the chamber was open. The values for the input and output voltage were read using an Goldstar 05-9020G analog oscilloscope. The frequency of the signal was varied between 3 and 4 MHz, and the input and output voltages were recorded. A plot was then made of gain as a function of frequency in order to approximately determine the quality (Q) factor of the resonance peak. This was done using 0.3, 0.6, 0.9, 1.2, and 1.6 μH for the primary coil inductance. A value of 1.2 μH gave the best resonance. Measurements were made in the same way replacing HP 3310A function generator with a HP 33120A function generator, Kalmus 155LCRH RF power amplifier, and LDG AT200PC antenna tuner. The results of this test are shown in Figure 25. After this frequency scan was recorded, the input voltage was increased to determine the largest voltage that can be applied to the dee. The test lead wire scorched with 3500 V on the dee, so the dee can withstand voltages at least this high without sparking.

This method of monitoring the RF voltage on the dee requires the system to be open to air. A pickup was designed which could be used when the system is evacuated. It was made of a length of wire which was bent into a shape that looked much like an electric stovetop heating element. The pickup was flush with the chamber wall when inserted into one of the ports. A voltage was induced in the pickup by the dee. The calibration factor the pickup scales the dee voltage by is about 50,000.

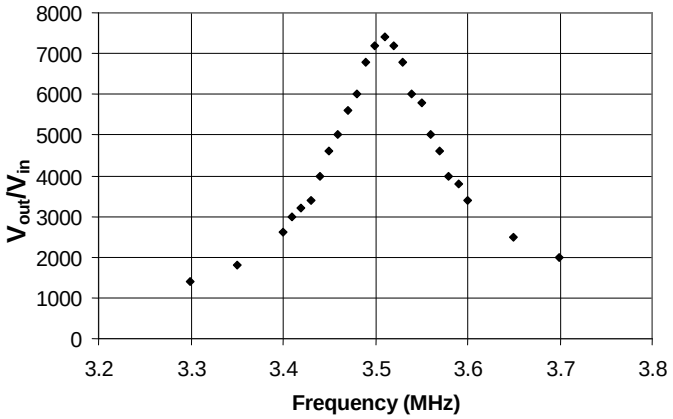

Figure 25. A typical full power resonance curve. These measurements were made with a primary coil inductance of 1.2 μH, secondary coil inductance of 21.4 μH, and dee capacitance 88.5 pF. The resonance is at 3.51 MHz, where an input voltage into the RF amplifier of 0.100 V peak-to-peak generates 740 V on the dee. Using Equation (25), the resonance should be at 3.65 MHz, however, this ignores the effect of the mutual inductance in the LC circuit. The quality factor of this curve is roughly 22, calculated by dividing the peak frequency by the bandwidth at half the maximum.

4.2 Resonance Results

Thus far, the Houghton College cyclotron has been operated successfully on only one occasion. Utilizing a scan from the Residual Gas Analyzer, it was determined that there was a sufficient quantity of residual hydrogen present in the chamber that could be accelerated. Hydrogen is used in manufacturing stainless steel, and it is believed the hydrogen in the chamber was a result from outgassing from the walls of the vacuum system. The gas handling system was not attached, and so no helium was present. The pressure was around 1.6×10^{-5} torr (a typical RGA scan is given in Figure 26).

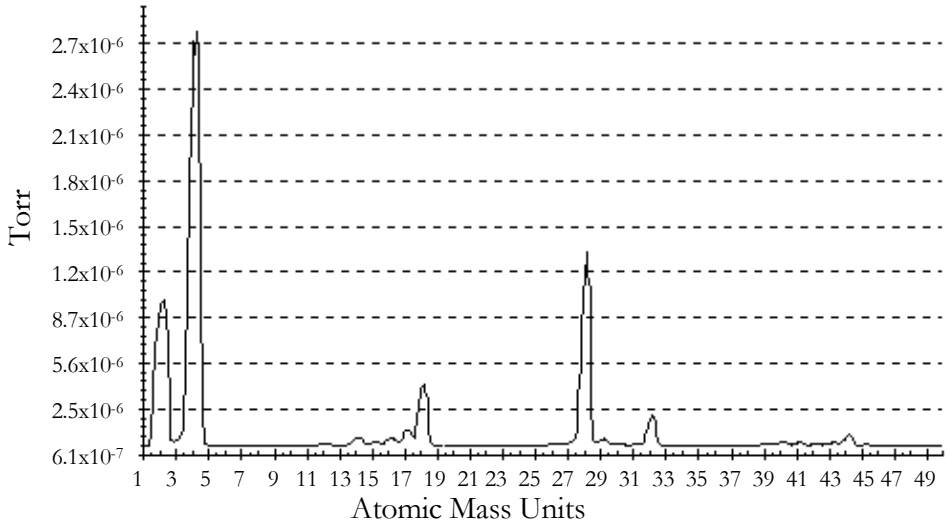

Figure 26. A Typical RGA scan in the Houghton College cyclotron. From left to right, the peaks represent the pressures of hydrogen (2 AMU), helium (4), water vapor (18), atmospheric nitrogen (28), and oxygen (32). The vertical scale shows the partial pressures of each gas. During this particular scan, the gas handling system was attached, and so helium is present.

To ionize the hydrogen, the filament was turned on, it began to glow at 1.5V, 1.6 A, and was turned as high as 2.0 A. The filament was floated at -100 V. The RF system was then turned on. The construction of the coils and dee stem at that time allowed for the function generator voltage to be multiplied by a factor of about 2800. This factor has a large uncertainty because at the time the high voltage probe used (Tektronics P6009) to test the RF system was not intended for high frequency AC signals. The function generator generated a 3.65 MHz signal with a 0.300 V peak-to-peak amplitude. Thus, the voltage on the dees was roughly 840 V peak-to-peak. At this point the magnet was turned on. The current supplied was 45 A, corresponding to a magnetic field strength of 1.07 T.

A resonance plot was made of beam current as a function of magnetic field, holding the frequency constant (3.65 MHz). Rearranging Equation 4 gives

$$B = \frac{2\pi m f_0}{q}, \tag{54}$$

where f_0 is the cyclotron frequency, and B is the magnetic field which would allow charged particles with mass m and charge q to be in resonance. As the magnetic field approached this value, the particles were accelerated, and a beam current was measured at the current collector. For ionized hydrogen at this frequency, the expected value of the magnetic field is 0.24 T.

To make this measurement, the magnetic field was measured with a Vernier Hall Effect probe. Because the maximum field rating of the probe was less than the field strength of the magnet, the probe was placed (using a ring stand and clamps) in the fringe field of the magnet, where the magnetic field strength would be a fraction of the center. The scale factor of the fringe field to the field at the center was found to be 173.6.

The beam current was measured by a Keithley 617 electrometer which provided a voltage output proportional to the beam current. This voltage was read by a Vernier voltage probe. Both the voltage probe and the Hall Effect probe were read into a Vernier LabPro interface. Rough calibration data were recorded; however, this was intended only as a preliminary scan. Unfortunately, after these data were recorded, a discharge from the dee to the chamber wall punctured the glass and epoxy insulation. Since then, the cyclotron has not been operational. The result of this measurement is displayed in Figure 27. This result is very similar in shape to a typical curve for the original cyclotron [53] (Figure 28), which demonstrated a sharp peak at resonance, with a shoulder the left of the peak.

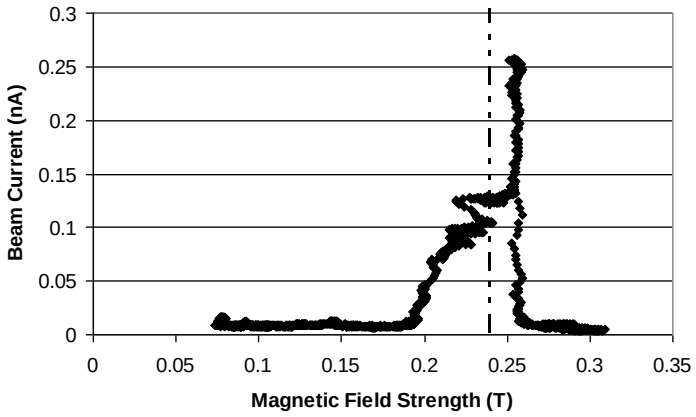

Figure 27. Resonance curve for hydrogen, with approximately 840 V peak to peak on the dees at a frequency of 3.65 MHz and a chamber pressure of 1.6 x 10^{-5}. The peak is approximately at 0.26 T. The dotted line represents the expected value (0.24 T) for the resonance according to the cyclotron Equation (54).The difference is most likely due to poor calibration. The oscillations in magnetic field measurements are likely due to the fact that the measurement depended very much on the probe's position, because the strength of the fringe field drops off quickly with radius. The probe was mounted using a ring stand and clamps, and it is likely that the table vibrated, possibly as a result of the forepump or other machinery.

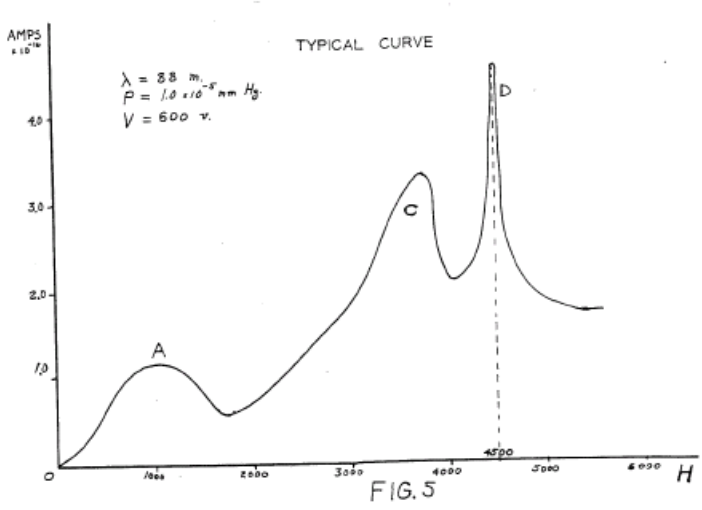

Figure 28. Typical resonance curve of the original cyclotron taken from M. Stanley Livingston's doctoral thesis [54]. The peak at D is the resonance peak. The hump at C is a result of particles that are slightly out of resonance. The peak at A is not present in the curve from the Houghton College cyclotron, possibly due to differences in design.

Chapter 5

CONCLUSION

The Houghton College Cyclotron, with the completion of the RF system, has been used to collect preliminary data, and has been shown to successfully accelerate protons. The resonance plot obtained was similar to a typical resonance curve for the first cyclotron described by M. Stanley Livingston. Currently, minor repairs are being made, including adding additional insulation to prevent further sparking, and using Quick Flange connections to replace the leaking foreline in the vacuum system. Also, an AEA Wireless VIA Bravo II network analyzer has been used to better measure the electric characteristics of the RF system.

The final goal of the cyclotron is neutron production and, because of the radiation hazard, the operator must control the cyclotron remotely. In the future, a control program will be written using Labview software, allowing the magnet power supply, ion gauge controller, RF function generator, antenna tuner, RGA, filament power supply, and electrometer to be controlled remotely through the college intranet. In addition, an adequate method of shielding from the neutrons will be devised. With these measures in place, the cyclotron will be fully operational.

References

1 E. Rutherford, Philos. Mag. **37**, 581 (1919).

2 E. Rutherford, Ibid. **37,** 581 (1919).

3 G. Gamow, Z. Phys. **52**, 510 (1928).

4 E. O. Lawrence and M. S. Livingston, Phys. Rev. **40**, 19 (1932).

5 E. O. Lawrence, Nobel Lecture, December 11, 1951.

6 M. A. Tuve, G. Breit, and L. R. Hafstad, Phys. Rev. **35**, 66 (1930).

7 M. Stanley Livingston and John P. Blewett, *Particle Accelerators.* (McGraw-Hill Book Company, New York, 1962), p. 18.

8 R. J. Van de Graaff, Phys Rev. **38**, 1919A (1931).

9 R.J. Van de Graaf, K.T. Compton, and L.C. Van Atta, Phys Rev. **43**, 149 (1933).

10 M. Stanley Livingston and John P. Blewett, *Particle Accelerators.* (McGraw-Hill Book Company, New York, 1962), p. 29.

11 G. Ising, Ark. Fys. **18**, 1 (1924).

12 G. Ising, Ibid. **18**, 2 (1924).

13 R. Wideröe, Archive Elektrotechnische. **21**, 387 (1928).

14 R. Wideröe, Ibid. **21**, 391 (1928).

15 E. O. Lawrence and D.H. Sloan, Phys. Rev. **38**, 2021 (1931).

16 E. O. Lawrence, Nobel Lecture, December 11, 1951.

17 E.O. Lawrence and N. Edlfesen, Science, **72**. 376 (1930).

18 M.S. Livingston, Ph.D. Thesis, University of California, 1931.

19 E. O. Lawrence and M. S. Livingston, Phys. Rev. **38**, 834 (1931).

20 E. O. Lawrence and M. S. Livingston, Phys. Rev. **40**, 19 (1932).

21 J. D. Cockcroft, and E. T. S. Walton, Proc. R. Soc. London, **136**, 619 (1932); **137**, p. 229 (1932).

22 E. O. Lawrence, M. S. Livingston, and M. G. White, Phys. Rev. **42**, 150 (1932).

23 E. O. Lawrence and M. S. Livingston, Phys. Rev. **45**, 608 (1934).

24 E. O. Lawrence and D. Cooksey, Phys Rev. **50**, 1131 (1936).

25 E. O. Lawrence, *et al.*, Phys. Rev. **56**, 124 (1939).

26 M. E. Rose and H. A. Bethe, Phys. Rev. **52**, 1254 (1937).

27 M. E. Rose, Phys. Rev. **53**, 392 (1938).

28 J.R. Richardson, *et al.*, Phys. Rev. **69**, 669 (1946).

29 D.W. Kerst, Nature, **157**, 90 (1946).

30 A.G. Ingalls, Sci. Am. **189** (3), p. 154 (1953).

31 B.V. Siegal and R.C. Sinnott, Phys. Today **1,** p. 10 (1948).

32 D. J. McGuire, Proc. Iowa Acad. Sci. **68**, 474 (1961).

33 J. J. Welch, K. J. Bertsche, P. J. Friedman, D. E. Morris and R. A. Muller, *California Institute of Technology Accelerator Mass Spectrometry Conference, February 15, 1986*. (1987).

34 K. J. Bertsche, C. A. Karadi, and R. A. Muller, Nucl. Instrum. Methods **301**, 358 (1991).

35 F. Niell. "Cyclotron Notes." (2002).

36 T. Feder, Phys Today **57,** 30 (2004).

37 "Rutger's Cyclotron." http://www.physics.rutgers.edu/cyclotron/welcome.shtml. (Viewed June 24, 2007).

38 J. Smith, undergraduate thesis, Knox College, 2001.

39 Jack T. Tanabe, *Iron Dominated Electromagnets: Design, Fabrication, Assembly, and Measurements*. (World Scientific, New Jersey, 2005) p. 230.

40 M. Stanley Livingston and John P. Blewett, *Particle Accelerators*. (McGraw-Hill Book Company, New York, 1962), p. 144.

41 M. Stanley Livingston and John P. Blewett, *Particle Accelerators*. (McGraw-Hill Book Company, New York, 1962), p. 149.

42 M. Stanley Livingston, *Particle Accelerators: A Brief History*. (Harvard University Press, Cambridge MA., 1969) p. 26-7.

43 M. Stanley Livingston and John P. Blewett, *Particle Accelerators*. (McGraw-Hill Book Company, New York, 1962), p. 129.

44 M. Stanley Livingston and John P. Blewett, *Particle Accelerators*. (McGraw-Hill Book Company, New York, 1962), p. 129.

45 M. E. Rose, Phys Rev. **53**, 715 (1938).

46 J. R. Richardson, *Particle Accel.Conf: IEEE 1991*. **1**, 48 (1991).

47 M. E. Rose, Phys. Rev. **53**, 392 (1938).

48 T. W. Koeth (unpublished).
http://www.physics.rutgers.edu/cyclotron/papers/12_inch_dee_voltage.pdf (2005). (Viewed June 24, 2007).

49 W. Bygrave, P. Treado, J. Lambert, *Accelerator Nuclear Physics*. (High Voltage Engineering Corporation, Burlington MA, 1970).

50 W. Bygrave, P. Treado, J. Lambert, *Accelerator Nuclear Physics*. (High Voltage Engineering Corporation, Burlington MA, 1970).

51 M.B. Chadwick, P. Oblozinsky, M. Herman *et al.*, "ENDF/B-VII.0: Next Generation Evaluated Nuclear Data Library for Nuclear Science and Technology", Nuclear Data Sheets, vol. 107, pp. 2931-3060, 2006.

52 M.S. Livingston, Ph.D. Thesis, University of California, 1931.

53 M.S. Livingston, Ph.D. Thesis, University of California, 1931.

54 M.S. Livingston, Ph.D. Thesis, University of California, 1931.